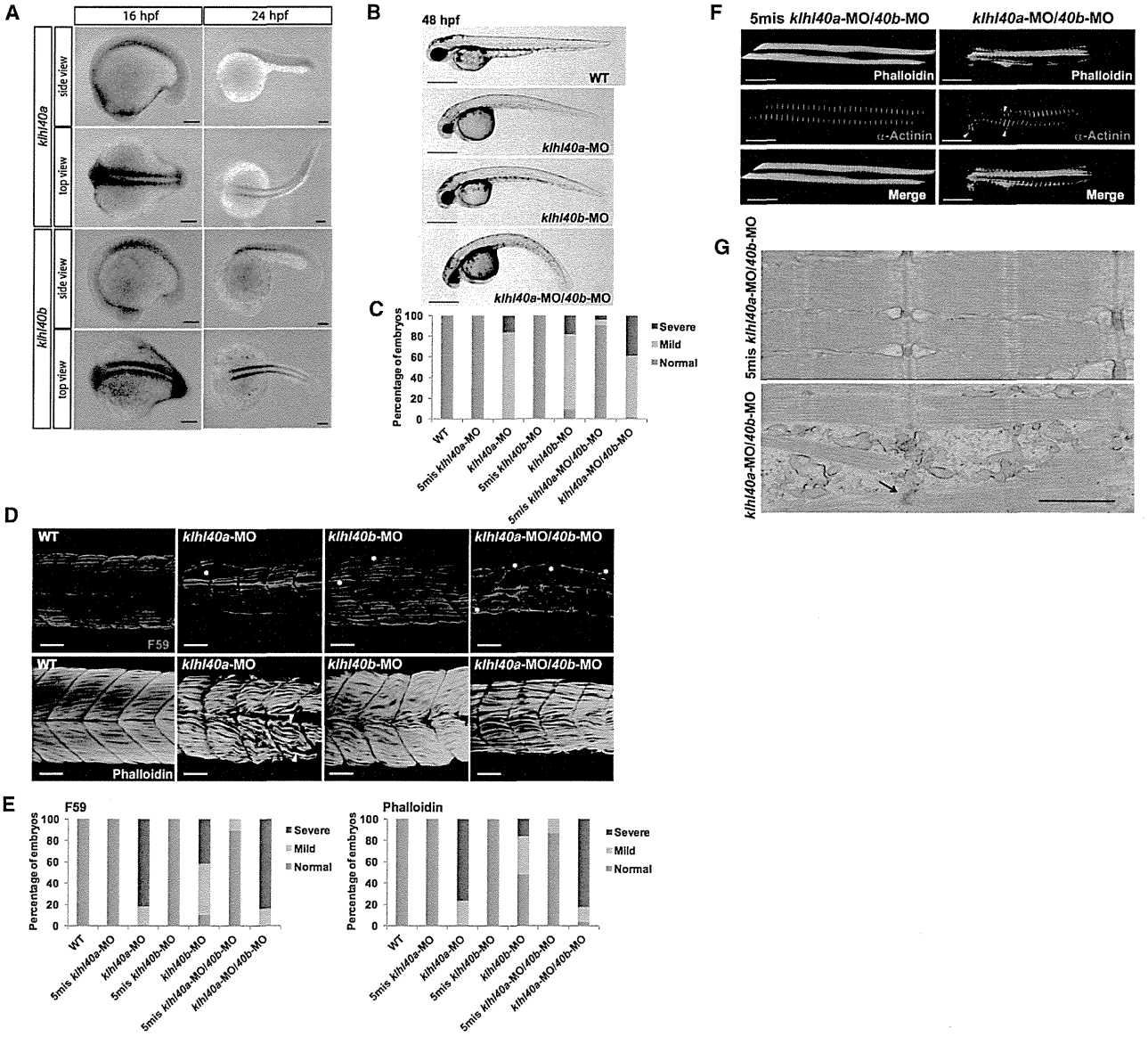

Figure 4. Expression and Function of *klhl40* in Zebrafish

(A) In situ hybridization demonstrates that expression of both *klhl40a* and *klhl40b* is restricted to the skeletal muscle at 16 and 24 hpf.

(B) Gross morphology of uninjected embryos (WT) and embryos injected with *klhl40a*-MO, *klhl40b*-MO, and *klhl40a*-MO/*40b*-MO. Lateral views of MO-injected embryos (4 ng) at 48 hpf are shown. Scale bars represent 500 μm.

(C) Percentage of embryos categorized in phenotypic classes after injection with the 5mis-MO control, *klhl40a*-MO, *klhl40b*-MO, or *klhl40a*-MO/*40b*-MO. We categorized the phenotypes at 48 hpf into normal (normal appearance), mild (curved trunk), and severe (tail defect and severe development delay) (n = 111–130).

(D) Knockdown of *klhl40a*, *klhl40b*, or both resulted in severe disruption of the skeletal muscle: fibers appeared wavy, and there were extensive gaps between fibers in contrast to the densely packed and aligned fibers of the controls. Maximum-intensity projection images from a confocal image series followed immunolabeling with a myosin antibody (F59, upper panels) at 36 hpf and F-actin (lower panels) at 72 hpf.

(E) Embryos injected with 5mis-MO, *klhl40a*-MO, *klhl40b*-MO, or *klhl40a*-MO/*40b*-MO were categorized phenotypically on the basis of the presence of myofiber detachment affecting one to two somites (mild) or multiple (three or more) somites (severe) (n = 25–44).

(F) Double-labeled immunofluorescence was performed on isolated myofibers from 72 hpf embryos with the use of phalloidin (green) and α-actinin (red). Frequent areas of aberrant α-actinin accumulation were detected in *klhl40a*-MO/*40b*-MO myofibers (arrowheads).

(G) Electron microscopy of 72 hpf myofibers. A 5mis-MO-injected embryo shows correctly aligned sarcomeres and T-tubules (upper panel). A *klhl40a*-MO/*40b*-MO-injected embryo (lower panel) shows disarranged myofibrils with widened Z-disks (arrow), but thin filament lengths are unchanged. The scale bar represents 0.7 μm.

We analyzed slow myofibers in more detail by immunostaining slow myosin heavy chains (Figure 4D, upper panels). *klhl40* morphants showed disruption of muscle patterning with an irregular, wavy appearance of the striated myofibers and extensive gaps between the myofibers (Figures 4D and 4E and Figure S10B) and a greatly

Table 2. Summary of Clinical Features of NEM Individuals with *KLHL40* Mutations

	Individuals with *KLHL40* Mutations (n = 32 Cases from 28 Families)	
	Total	**Percentage**
Family history	17/28	60.7%
Consanguinity	10/28	35.7%
Prenatal Period		
Prenatal symptoms	24/29	82.8%
Fetal akinesia or hypokinesia	16/21	76.2%
Polyhydramnios	14/29	48.3%
Neonatal Period		
Respiratory function		
respiratory failure	28/29	96.6%
requiring ventilation	11/29	37.9%
Facial involvement	26/26	100%
weakness	23/23	100%
ophthalmoparesis	4/23	17.4%
mild dysmorphology	15/15	100%
Dysphagia	23/24	95.8%
with tube feeding or gastrostomy	13/24	54.2%
Muscle weakness	29/29	100.0%
with no spontaneous antigravity movements	13/29	44.8%
Contracture(s)	24/27	88.9%
Pathological fracture(s)	10/19	52.6%
Average age at death	5 months (n = 14)	
Average gestation age at birth	37 weeks (n = 27)	
Average birth weight	2,558 g (n = 26)	

Total numbers were calculated as the number of individuals with the clinical features over the total number of individuals whose medical records were available for each category.

diminished birefringence (Figure S10C). Isolated myofibers from *klhl40a*-MO/*40b*-MO fish, coimmunostained with phalloidin and an α-actinin antibody (Z-disk), showed disorganized and irregular patterns with small aggregates of α-actinin, suggesting nemaline bodies (Figure 4F). Aggregation of Z-disk material was also confirmed by immunostaining for filamin C in *klhl40a*-MO/*40b*-MO fish (Figure S11). Electron-microscopic analysis revealed disarranged myofibrils with widened Z-disks (Figure 4G). Fish injected with *klhl40a*-MO, *klhl40b*-MO, *klhl40b*-MO2, or *klhl40a*-MO/*40b*-MO2 (double morpholinos) exhibited sporadic muscle tremors, and coordinated swimming behavior was not observed (Movies S1 and S2). These results suggest that Klhl40a and Klhl40b are required for muscle development and function and that loss of either isoform in the early embryo is sufficient to impair normal mobility.

Detailed clinical records were collected and analyzed for 32 affected individuals from the 28 unrelated kindreds afflicted with *KLHL40* mutations. These individuals were from various ethnicities, such as European, Middle and Near Eastern, or Asian. Clinical features of individuals with *KLHL40* mutations were severe and distinctive (Table 2 and Table S3). Eighty-three percent of affected individuals showed prenatal symptoms, and 76% displayed fetal akinesia or hypokinesia. Most persons had severe respiratory compromise (97%), and approximately a third required ventilatory support (38%). Almost all affected individuals (96%) also had swallowing problems, and half required tube feeding or gastrostomy. Muscle weakness was severe. Forty-five percent of individuals had no spontaneous antigravity movement. Seventeen percent of affected individuals were also noted to have ophthalmoparesis, a relatively rare symptom in NEM. Multiple joint contractures and pathological bone fracture were other common features. Dysmorphic facial features and deformities of the chest, spine, fingers, and feet were also frequent. The average age of death was 5 months. Many families, including a previously described family (family 30 herein, cases 2–6 in Lammens et al.),[11] were consanguineous.

We further evaluated whether there are any genotype-phenotype correlations in *KLHL40*-associated NEM. We compared the clinical features of individuals according to the type of mutation they had (either two truncating mutations, one truncating mutation and one missense mutation, or two missense mutations) and the pattern of mutations (homozygous or compound heterozygous). No significant differences in frequencies of these clinical features were observed (data not shown). We also compared the clinical features of persons with the recurrent c.1582G>A genotype (either with this mutation [genotype G/A or A/A as group A] or without [genotype G/G as group G]). Prenatal symptoms, including fetal akinesia or hypokinesia, were frequently observed (73.3% in group A versus 92.9% in group G). Respiratory failure was common in both groups (100% in group A versus 92.9% in group G), but there were significantly fewer individuals requiring ventilation in group A than in group G (20.0% in group A versus 57.1% in group G; $p = 0.047$). Dysphagia was also common in both groups (100% in group A versus 90.0% in group G), but there were fewer persons requiring tube feeding or gastrostomy in group A than in group G, although the difference was not significant (42.9% in group A versus 70.0% in group G; $p = 0.127$). Facial weakness was observed in all affected individuals in both groups, but fewer individuals in group A had ophthalmoparesis (7.7% in group A versus 30.0% in group G; $p = 0.281$). All persons also had muscle weakness, but significantly fewer individuals in group A had the most severe form of muscle weakness with no antigravity movements (20.0% in group A versus 71.4% in group G; $p = 0.018$). Significantly fewer affected individuals in group A were deceased at the time of study than in group G (23.5% in group A versus 71.4% in group G; $p = 0.012$;

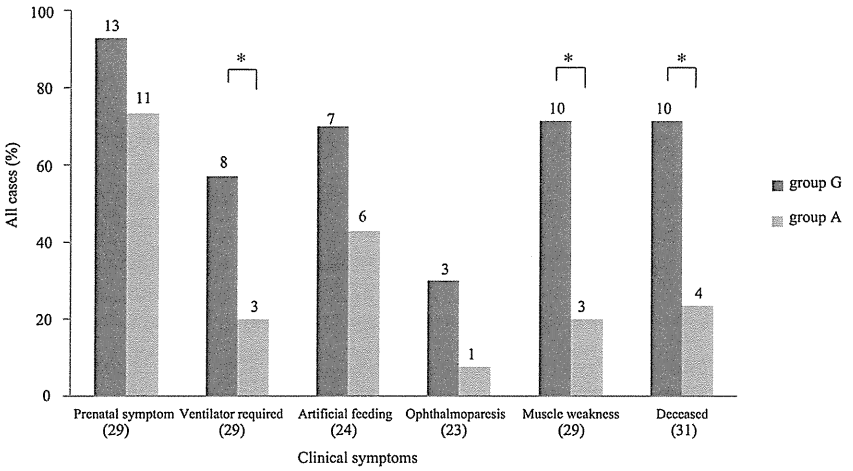

Figure 5. Correlation between the c.1582G>A (p.Glu528Lys) Mutation and Clinical Features

The clinical characteristics of NEM are shown for the two groups of affected individuals (32 total), either with the c.1582G>A (p.Glu528Lys) mutation (as group A) or without it (as group G). The numbers of total affected individuals with clinical records regarding either the presence or the absence of each characteristic are indicated below the bars, and the numbers of affected individuals in each group are indicated above the respective bars. Labels on the x axis are as follows: prenatal symptoms, individuals demonstrating either fetal akinesia or hypokinesia, polyhydramnios, or fetal edema or effusion; ventilator required, individuals with respiratory failure requiring ventilation; artificial feeding, dysphagia-affected persons requiring tube feeding or gastrostomy; ophthalmoparesis, individuals with ophthalmoparesis along with facial weakness; muscle weakness, individuals with the most severe form of muscle weakness and demonstrating no antigravitory movement; and deceased, individuals who were deceased at the time of study. Asterisks indicate that statistical significance was observed.

odds ratio = 8.125; 95% confidence interval = 1.62–40.75) (Figure 5). We further compared the clinical features of individuals of different ethnicities (either European or Asian descent) according to the c.1582G>A genotype, and similar tendencies were demonstrated (data not shown). There was, however, great variation in severity for individuals with or without the c.1582G>A genotype.

Discussion

We have described the identification of recessive *KLHL40* mutations in individuals with severe NEM from 28 unrelated families of various ethnicities. The c.1582G>A mutation was the most frequently detected mutation and was found in Japanese, Kurdish, and Turkish persons. However, comparison of haplotypes between a Japanese family and a Turkish family suggested that the mutation arose independently in these ethnic groups. We have shown several lines of evidence of the pathogenicity of the *KLHL40* mutations. The missense mutations occurred mostly in conserved functional domains within KLHL40, and they were predicted to destabilize the intramolecular interactions and thus impair protein stability. This was corroborated by the absence of KLHL40 even in the skeletal muscle of individuals harboring two missense mutations. We have established a locus-specific database for *KLHL40* mutations at the Leiden Muscular Dystrophy Pages.

Expression of KLHL40 in fetal and adult skeletal muscle indicates that KLHL40 plays a role in both myogenesis and mature muscle. KLHL40 appears to be more abundant in fetal skeletal muscle than in postnatal skeletal muscle and most likely accounts for the prevalence of in utero presentations in this NEM cohort. Perhaps KLHL40 is more important for myogenesis than for muscle maintenance; this could account for the fact that the disease ranges so much in severity, from some individuals' dying within hours of being born to others' surviving into adolescence. Our zebrafish studies have demonstrated that Klhl40a and Klhl40b are not required for the specification of muscle cells but rather for muscle patterning and function and that loss of either isoform in the early embryo is sufficient to impair normal mobility, supporting the involvement of KLHL40 in NEM-associated fetal akinesia. It has previously been suggested that KLHL40 is also important for muscle maintenance through the process of degeneration and regeneration.[29,30] *Klhl40* is upregulated in myogenic precursors after cardiotoxin injury of mouse skeletal muscle, supporting a role for *Klhl40* in the response to muscle damage.[29] Studies of cattle muscle have shown increased *Klhl40* expression in another catabolic process, undernutrition, further suggesting a role for *KLHL40* in the stress response.[30]

KLHL40 belongs to the superfamily of kelch-repeat-containing proteins that form characteristic β-propeller structures,[31] which bind substrate proteins and are involved in a wide variety of functions. In humans, 71 kelch-repeat-containing proteins have been identified.[31] The majority contain an N-terminal BTB domain (also known as the POZ [poxvirus and zinc finger] domain) and a BACK motif. Proteins containing both a BTB domain and a kelch repeat have previously been implicated in neuromuscular disease. A dominant *KLHL9* mutation causes an early-onset distal myopathy (distal myopathy 1 [MIM 160500]),[32] and dominant *KBTBD13* mutations cause nemaline myopathy with cores (MIM 609273).[9] We now show that *KLHL40*, encoding KLHL40, which contains both a BTB domain and a kelch repeat, is associated with autosomal-recessive neuromuscular disease. BTB domains function as substrate-specific adaptors for cullin 3 (Cul3),[33,34] a component of the E3-ubiquitin-ligase complex. Both KLHL9 and KBTBD13 bind Cul3.[10,32] MuRF1,

an E3-ubiquitin ligase, is known to be recruited to M-line titin and is thought to modulate myofibrillar turnover and the trophic state of muscle.[35] KLHL40 appears to be present at the A-band and might be similarly involved through the ubiquitin-proteasome pathway.

We have characterized the severe and distinctive features of this disease as fetal akinesia or hypokinesia during the prenatal period, respiratory failure and swallowing difficulty at birth, contractures and fractures along with dysmorphic features, and in most cases, early death. We have also shown that persons with the recurrent c.1582G>A mutation tend to have relatively milder symptoms compared to those of individuals without c.1582G>A. However, the severity of the disease in persons with or without the c.1582G>A genotype varied greatly (for example, from death at 20 days to still being alive at 11 years for persons homozygous for the c.1582G>A genotype), suggesting modifying factors.

Fetal akinesias are clinically and genetically heterogeneous, and the majority of cases still remain genetically unsolved.[36] Primary muscle diseases account for up to 50% of such syndromes.[37] On the basis of our study, *KLHL40* mutations cause a significant proportion of severe NEM cases of fetal akinesia sequence and the disease shows worldwide prevalence. *KLHL40* should be considered when a clinician encounters an individual presenting with prenatal symptoms, such as fetal akinesia or hypokinesia, or clinical features and/or pathology of severe NEM at birth (especially miliary NEM, which was present in at least 20% of our *KLHL40*-mutation cases), along with an autosomal-recessive pattern of family history. Fractures are a relatively frequent presentation within this cohort, unlike other NEM cohorts, and should also be used for directing genetic screening of *KLHL40*. We show that KLHL40 immunohistochemistry, immunoblotting, or genetic screening will identify the disease and thus allow genetic counseling for the affected individual's family.

In conclusion, this study associates loss-of-function *KLHL40* mutations with severe, often in utero, NEM. Many probands who do not harbor *KLHL40* mutations present with NEM in utero, suggesting further genetic heterogeneity. Clarification of KLHL40 function and interactions might lead to a greater understanding of the pathogenesis of disease, the identification of other candidates for this severe form of NEM, and the investigation of possible therapies.

Supplemental Data

Supplemental Data include 11 figures, three tables, and two movies and can be found with this article online at http://www.cell.com/AJHG.

Acknowledgments

This research was supported by the National Health and Medical Research Council of Australia (fellowships APP1035955 to G.R. and APP1002147 to N.G.L. and grant APP1022707) and Association Francaise contre les Myopathies (AFM; AFM15734). E.T. and K.S.Y. are supported by university postgraduate awards. This work received grants from the Ministry of Health, Labour, and Welfare (N. Miyake, H.S., and N. Matsumoto), Japan Science and Technology Agency (N. Matsumoto), Strategic Research Program for Brain Sciences (E.K. and N. Matsumoto), and Takeda Science Foundation (N. Miyake and N. Matsumoto) and Grants-in-Aid for Scientific Research on Innovative Areas (Transcription Cycle) from the Ministry of Education, Culture, Sports, Science, and Technology of Japan (N. Miyake and N. Matsumoto) and for Scientific Research from the Japan Society for the Promotion of Science (N. Miyake, H.S., and N. Matsumoto). The A.H.B. laboratory was supported by the National Institutes of Health (R01-AR044345) and the Muscular Dystrophy Association (MDA201302). O.C. is a Dubai Harvard Foundation for Medical Research Fellow and a grantee of the Schlumberger Foundation Faculty for the Future Program. E.B. is supported by grants from Telethon (GUP08005) and the Ministry of Health on Congenital Myopathies. F.M. is supported by the Great Ormond Street Children's Charity and National Specialist Commissioning Group. P.V. and V.-L.L. were supported by grants to C.W.-P. by the AFM, Sigrid Jusélius Foundation, Academy of Finland, Finska Läkaresällskapet, and Medicinska Understödsföreningen Liv och Hälsa r.f. R.V. is supported by a Monash Graduate Research Scholarship and a Faculty of Science Dean's International Postgraduate Research Scholarship.

Received: March 15, 2013
Revised: April 25, 2013
Accepted: May 3, 2013
Published: June 6, 2013

Web Resources

The URLs for data presented herein are as follows:

1000 Genomes Project, http://www.1000genomes.org/
dbSNP, http://www.ncbi.nlm.nih.gov/projects/SNP/
Leiden Open Variation Database, www.LOVD.nl/KLHL40
NHLBI Exome Sequencing Project (ESP) Exome Variant Server, http://evs.gs.washington.edu/EVS/
Online Mendelian Inheritance in Man (OMIM), http://www.omim.org
PyMOL, http://www.pymol.org
RefSeq, http://www.ncbi.nlm.nih.gov/RefSeq

References

1. Nance, J.R., Dowling, J.J., Gibbs, E.M., and Bönnemann, C.G. (2012). Congenital myopathies: an update. Curr. Neurol. Neurosci. Rep. *12*, 165–174.
2. Nowak, K.J., Davis, M.R., Wallgren-Pettersson, C., Lamont, P.J., and Laing, N.G. (2012). Clinical utility gene card for: nemaline myopathy. Eur. J. Hum. Genet. *20*. Published online April 18, 2012. http://dx.doi.org/10.1038/ejhg.2012.70.
3. Nowak, K.J., Wattanasirichaigoon, D., Goebel, H.H., Wilce, M., Pelin, K., Donner, K., Jacob, R.L., Hübner, C., Oexle, K., Anderson, J.R., et al. (1999). Mutations in the skeletal muscle alpha-actin gene in patients with actin myopathy and nemaline myopathy. Nat. Genet. *23*, 208–212.
4. Agrawal, P.B., Greenleaf, R.S., Tomczak, K.K., Lehtokari, V.L., Wallgren-Pettersson, C., Wallefeld, W., Laing, N.G., Darras,

B.T., Maciver, S.K., Dormitzer, P.R., and Beggs, A.H. (2007). Nemaline myopathy with minicores caused by mutation of the CFL2 gene encoding the skeletal muscle actin-binding protein, cofilin-2. Am. J. Hum. Genet. *80*, 162–167.

5. Lehtokari, V.L., Pelin, K., Sandbacka, M., Ranta, S., Donner, K., Muntoni, F., Sewry, C., Angelini, C., Bushby, K., Van den Bergh, P., et al. (2006). Identification of 45 novel mutations in the nebulin gene associated with autosomal recessive nemaline myopathy. Hum. Mutat. *27*, 946–956.
6. Johnston, J.J., Kelley, R.I., Crawford, T.O., Morton, D.H., Agarwala, R., Koch, T., Schäffer, A.A., Francomano, C.A., and Biesecker, L.G. (2000). A novel nemaline myopathy in the Amish caused by a mutation in troponin T1. Am. J. Hum. Genet. *67*, 814–821.
7. Donner, K., Ollikainen, M., Ridanpää, M., Christen, H.J., Goebel, H.H., de Visser, M., Pelin, K., and Wallgren-Pettersson, C. (2002). Mutations in the beta-tropomyosin (TPM2) gene—a rare cause of nemaline myopathy. Neuromuscul. Disord. *12*, 151–158.
8. Laing, N.G., Wilton, S.D., Akkari, P.A., Dorosz, S., Boundy, K., Kneebone, C., Blumbergs, P., White, S., Watkins, H., Love, D.R., et al. (1995). A mutation in the alpha tropomyosin gene TPM3 associated with autosomal dominant nemaline myopathy. Nat. Genet. *9*, 75–79.
9. Sambuughin, N., Yau, K.S., Olivé, M., Duff, R.M., Bayarsaikhan, M., Lu, S., Gonzalez-Mera, L., Sivadorai, P., Nowak, K.J., Ravenscroft, G., et al. (2010). Dominant mutations in KBTBD13, a member of the BTB/Kelch family, cause nemaline myopathy with cores. Am. J. Hum. Genet. *87*, 842–847.
10. Sambuughin, N., Swietnicki, W., Techtmann, S., Matrosova, V., Wallace, T., Goldfarb, L., and Maynard, E. (2012). KBTBD13 interacts with Cullin 3 to form a functional ubiquitin ligase. Biochem. Biophys. Res. Commun. *421*, 743–749.
11. Lammens, M., Moerman, P., Fryns, J.P., Lemmens, F., van de Kamp, G.M., Goemans, N., and Dom, R. (1997). Fetal akinesia sequence caused by nemaline myopathy. Neuropediatrics *28*, 116–119.
12. Lacson, A.G., Donaldson, G., Barness, E.G., Ranells, J.D., and Pomerance, H.H. (2002). Infant with high arched palate, bell-shaped chest, joint contractures, and intrauterine fractures. Pediatr. Pathol. Mol. Med. *21*, 569–584.
13. Ravenscroft, G., Jackaman, C., Bringans, S., Papadimitriou, J.M., Griffiths, L.M., McNamara, E., Bakker, A.J., Davies, K.E., Laing, N.G., and Nowak, K.J. (2011). Mouse models of dominant ACTA1 disease recapitulate human disease and provide insight into therapies. Brain *134*, 1101–1115.
14. Abecasis, G.R., Cherny, S.S., Cookson, W.O., and Cardon, L.R. (2002). Merlin—rapid analysis of dense genetic maps using sparse gene flow trees. Nat. Genet. *30*, 97–101.
15. Ravenscroft, G., Thompson, E.M., Todd, E.J., Yau, K.S., Kresoje, N., Sivadorai, P., Friend, K., Riley, K., Manton, N.D., Blumbergs, P., et al. (2013). Whole exome sequencing in foetal akinesia expands the genotype-phenotype spectrum of GBE1 glycogen storage disease mutations. Neuromuscul. Disord. *23*, 165–169.
16. Wang, K., Li, M., and Hakonarson, H. (2010). ANNOVAR: functional annotation of genetic variants from high-throughput sequencing data. Nucleic Acids Res. *38*, e164.
17. Harrow, J., Denoeud, F., Frankish, A., Reymond, A., Chen, C.K., Chrast, J., Lagarde, J., Gilbert, J.G., Storey, R., Swarbreck, D., et al. (2006). GENCODE: producing a reference annotation for ENCODE. Genome Biol. *7(Suppl 1)*, S4.1–S4.9.
18. Garritano, S., Gemignani, F., Voegele, C., Nguyen-Dumont, T., Le Calvez-Kelm, F., De Silva, D., Lesueur, F., Landi, S., and Tavtigian, S.V. (2009). Determining the effectiveness of High Resolution Melting analysis for SNP genotyping and mutation scanning at the TP53 locus. BMC Genet. *10*, 5.
19. Doi, H., Yoshida, K., Yasuda, T., Fukuda, M., Fukuda, Y., Morita, H., Ikeda, S., Kato, R., Tsurusaki, Y., Miyake, N., et al. (2011). Exome sequencing reveals a homozygous SYT14 mutation in adult-onset, autosomal-recessive spinocerebellar ataxia with psychomotor retardation. Am. J. Hum. Genet. *89*, 320–327.
20. Schymkowitz, J., Borg, J., Stricher, F., Nys, R., Rousseau, F., and Serrano, L. (2005). The FoldX web server: an online force field. Nucleic Acids Res. *33*(Web Server issue), W382–W388.
21. Van Durme, J., Delgado, J., Stricher, F., Serrano, L., Schymkowitz, J., and Rousseau, F. (2011). A graphical interface for the FoldX forcefield. Bioinformatics *27*, 1711–1712.
22. Nowak, K.J., Ravenscroft, G., Jackaman, C., Filipovska, A., Davies, S.M., Lim, E.M., Squire, S.E., Potter, A.C., Baker, E., Clément, S., et al. (2009). Rescue of skeletal muscle alpha-actin-null mice by cardiac (fetal) alpha-actin. J. Cell Biol. *185*, 903–915.
23. Ravenscroft, G., Nowak, K.J., Jackaman, C., Clément, S., Lyons, M.A., Gallagher, S., Bakker, A.J., and Laing, N.G. (2007). Dissociated flexor digitorum brevis myofiber culture system—a more mature muscle culture system. Cell Motil. Cytoskeleton *64*, 727–738.
24. Ruparelia, A.A., Zhao, M., Currie, P.D., and Bryson-Richardson, R.J. (2012). Characterization and investigation of zebrafish models of filamin-related myofibrillar myopathy. Hum. Mol. Genet. *21*, 4073–4083.
25. Zeller, J., Schneider, V., Malayaman, S., Higashijima, S., Okamoto, H., Gui, J., Lin, S., and Granato, M. (2002). Migration of zebrafish spinal motor nerves into the periphery requires multiple myotome-derived cues. Dev. Biol. *252*, 241–256.
26. Abecasis, G.R., Auton, A., Brooks, L.D., DePristo, M.A., Durbin, R.M., Handsaker, R.E., Kang, H.M., Marth, G.T., and McVean, G.A.; 1000 Genomes Project Consortium. (2012). An integrated map of genetic variation from 1,092 human genomes. Nature *491*, 56–65.
27. Kimura, M., and Ota, T. (1973). The age of a neutral mutant persisting in a finite population. Genetics *75*, 199–212.
28. Guerois, R., Nielsen, J.E., and Serrano, L. (2002). Predicting changes in the stability of proteins and protein complexes: a study of more than 1000 mutations. J. Mol. Biol. *320*, 369–387.
29. Embree, E.J. (2007). The identification and characterization of MKRP, a novel kelch related protein. PhD Thesis, Graduate School of Biomedical Sciences, The University of Texas Southwestern Medical Center at Dallas, Dallas, TX. http://repositories.tdl.org/utswmed-ir/bitstream/handle/2152.5/226/embreelaurence.pdf?sequence=3.
30. Lehnert, S.A., Byrne, K.A., Reverter, A., Nattrass, G.S., Greenwood, P.L., Wang, Y.H., Hudson, N.J., and Harper, G.S. (2006). Gene expression profiling of bovine skeletal muscle in response to and during recovery from chronic and severe undernutrition. J. Anim. Sci. *84*, 3239–3250.
31. Prag, S., and Adams, J.C. (2003). Molecular phylogeny of the kelch-repeat superfamily reveals an expansion of BTB/kelch proteins in animals. BMC Bioinformatics *4*, 42.
32. Cirak, S., von Deimling, F., Sachdev, S., Errington, W.J., Herrmann, R., Bönnemann, C., Brockmann, K., Hinderlich, S.,

Lindner, T.H., Steinbrecher, A., et al. (2010). Kelch-like homologue 9 mutation is associated with an early onset autosomal dominant distal myopathy. Brain *133*, 2123–2135.
33. Furukawa, M., He, Y.J., Borchers, C., and Xiong, Y. (2003). Targeting of protein ubiquitination by BTB-Cullin 3-Roc1 ubiquitin ligases. Nat. Cell Biol. *5*, 1001–1007.
34. Canning, P., Cooper, C.D., Krojer, T., Murray, J.W., Pike, A.C., Chaikuad, A., Keates, T., Thangaratnarajah, C., Hojzan, V., Marsden, B.D., et al. (2013). Structural basis for Cul3 protein assembly with the BTB-Kelch family of E3 ubiquitin ligases. J. Biol. Chem. *288*, 7803–7814.
35. Mrosek, M., Labeit, D., Witt, S., Heerklotz, H., von Castelmur, E., Labeit, S., and Mayans, O. (2007). Molecular determinants for the recruitment of the ubiquitin-ligase MuRF-1 onto M-line titin. FASEB J. *21*, 1383–1392.
36. Ravenscroft, G., Sollis, E., Charles, A.K., North, K.N., Baynam, G., and Laing, N.G. (2011). Fetal akinesia: review of the genetics of the neuromuscular causes. J. Med. Genet. *48*, 793–801.
37. Quinn, C.M., Wigglesworth, J.S., and Heckmatt, J. (1991). Lethal arthrogryposis multiplex congenita: a pathological study of 21 cases. Histopathology *19*, 155–162.

ARTICLE IN PRESS

JNS-12224; No of Pages 6

Journal of the Neurological Sciences xxx (2012) xxx–xxx

Contents lists available at SciVerse ScienceDirect

Journal of the Neurological Sciences

journal homepage: www.elsevier.com/locate/jns

Heterozygous UDP-GlcNAc 2-epimerase and *N*-acetylmannosamine kinase domain mutations in the *GNE* gene result in a less severe GNE myopathy phenotype compared to homozygous *N*-acetylmannosamine kinase domain mutations

Madoka Mori-Yoshimura [a,*], Kazunari Monma [b], Naoki Suzuki [c], Masashi Aoki [c], Toshihide Kumamoto [d], Keiko Tanaka [e], Hiroyuki Tomimitsu [f], Satoshi Nakano [g], Masahiro Sonoo [h], Jun Shimizu [i], Kazuma Sugie [j], Harumasa Nakamura [a,k], Yasushi Oya [a], Yukiko K. Hayashi [b], May Christine V. Malicdan [b], Satoru Noguchi [b], Miho Murata [a], Ichizo Nishino [b]

[a] *Department of Neurology, National Center Hospital, National Center of Neurology and Psychiatry, 4-1-1 Ogawahigashi, Kodaira, Tokyo 187-8551, Japan*
[b] *Department of Neuromuscular Research, National Institute of Neuroscience, National Center of Neurology and Psychiatry, 4-1-1 Ogawahigashi, Kodaira, Tokyo 187-8502, Japan*
[c] *Department of Neurology, Tohoku University School of Medicine, 1-1 Seiryo, Aoba-ku, Sendai 980-8574, Japan*
[d] *Department of Internal Medicine 3, Faculty of Medicine, Oita University, 1-1 Idaigaoka, Hasama, Yufu-shi, Oita 879-5593, Japan*
[e] *Department of Neurology, Kanazawa Medical University, 1-1 Daigaku, Uchinadamachi, Kahoku-gun, Ishikawa, 920-0214, Japan*
[f] *Department of Neurology and Neurological Science, Graduate School, Tokyo Medical and Dental University, Yushima 1-5-45, Bunkyo-ku, Tokyo 113-8519, Japan*
[g] *Department of Neurology, Osaka City General Hospital, 2-13-22, Miyakojimahonndoori, Miyakojima-ku, Osaka534-0021, Japan*
[h] *Department of Neurology, Teikyo University School of Medicine, Kaga 2-11-1, Itabashi-ku, Tokyo 173-8605, Japan*
[i] *Department of Neurology, Division of Neuroscience, Graduate School of Medicine, University of Tokyo, 7-3-1 Hongo, Bunkyo-ku, Tokyo 113-8655, Japan*
[j] *Department of Neurology, Nara Medical University School of Medicine, 840 Shijo, Kashihara, Nara 634-8521, Japan*
[k] *Clinical Trial Division, Division of Clinical Research, National Center Hospital of Neurology and Psychiatry, 4-1-1 Ogawahigashi, Kodaira, Tokyo 187-8551, Japan*

ARTICLE INFO

Article history:
Received 10 January 2012
Received in revised form 20 March 2012
Accepted 21 March 2012
Available online xxxx

Keywords:
GNE myopathy
Distal myopathy with rimmed vacuoles
Hereditary inclusion body myopathy
Glucosamine (UDP-N-acetyl)-2-epimerase/*N*-acetylmannosamine kinase
(UDP-N-acetyl)-2-epimerase domain
N-acetylmannosamine kinase domain
Questionnaire
Natural history

ABSTRACT

Background: Glucosamine (UDP-N-acetyl)-2-epimerase/*N*-acetylmannosamine kinase (GNE) myopathy, also called distal myopathy with rimmed vacuoles (DMRV) or hereditary inclusion body myopathy (HIBM), is a rare, progressive autosomal recessive disorder caused by mutations in the *GNE* gene. Here, we examined the relationship between genotype and clinical phenotype in participants with GNE myopathy.
Methods: Participants with GNE myopathy were asked to complete a questionnaire regarding medical history and current symptoms.
Results: A total of 71 participants with genetically confirmed GNE myopathy (27 males and 44 females; mean age, 43.1 ± 13.0 (mean ± SD) years) completed the questionnaire. Initial symptoms (*e.g.*, foot drop and lower limb weakness) appeared at a mean age of 24.8 ± 8.3 years. Among the 71 participants, 11 (15.5%) had the ability to walk, with a median time to loss of ambulation of 17.0 ± 2.1 years after disease onset. Participants with a homozygous mutation (p.V572L) in the *N*-acetylmannosamine kinase domain (KD/KD participants) had an earlier disease onset compared to compound heterozygous participants with mutations in the uridine diphosphate-N-acetylglucosamine (UDP-GlcNAc) 2-epimerase and *N*-acetylmannosamine kinase domains (ED/KD participants; 26.3 ± 7.3 vs. 21.2 ± 11.1 years, respectively). KD/KD participants were more frequently non-ambulatory compared to ED/KD participants at the time of survey (80% vs. 50%). Data were verified using medical records available from 17 outpatient participants.
Conclusions: Homozygous KD/KD participants exhibited a more severe phenotype compared to heterozygous ED/KD participants.

1. Introduction

Glucosamine (UDP-N-acetyl)-2-epimerase/*N*-acetylmannosamine kinase (GNE) myopathy, also known as distal myopathy with rimmed vacuoles (DMRV), Nonaka myopathy (MIM: 605820) or hereditary inclusion body myopathy (HIBM; MIM: 600737), is an early adult-onset, progressive myopathy that affects the tibialis anterior muscle, but spares quadriceps femoris muscles [1,2]. The disease is caused by a mutation in the *GNE* gene, which encodes a bifunctional enzyme [uridine diphosphate-*N*-acetylglucosamine (UDP-GlcNAc) 2-epimerase (GNE) and *N*-acetylmannosamine kinase (MNK)] known to catalyze two rate-limiting reactions involved in cytosolic sialic acid synthesis [3–7]. Mutations in the *GNE* gene result in decreased enzymatic activity *in vitro* by 30–90% [7–10]. Therefore, hyposialylation is thought to

* Corresponding author. Tel.: +81 42 341 2711; fax: +81 42 346 1852.
E-mail address: yoshimur@ncnp.go.jp (M. Mori-Yoshimura).

0022-510X/$ – see front matter © 2012 Elsevier B.V. All rights reserved.
doi:10.1016/j.jns.2012.03.016

Please cite this article as: Mori-Yoshimura M, et al, Heterozygous UDP-GlcNAc 2-epimerase and *N*-acetylmannosamine kinase domain mutations in the *GNE*..., J Neurol Sci (2012), doi:10.1016/j.jns.2012.03.016

contribute to the pathogenesis of GNE myopathy. This is supported by the myopathic phenotype associated with a mouse model expressing the human D176V mutant GNE protein (GNE−/−hGNED176V-Tg) [11]. Muscle atrophy and weakness are prevented by oral treatment with sialic acid metabolites in this mouse model [12].

A phase I clinical trial using oral sialic acid therapy has recently been performed in Japan for the treatment of GNE myopathy (ClinicalTrials.gov; NCT01236898). A similar phase I study is currently underway in the United States (ClinicalTrials.gov; NCT01359319). Natural history and genotype–phenotype correlations need to be established for a successful phase II clinical trial for the treatment of GNE myopathy. However, only a small number of studies have been conducted that review the natural course of this disease. In addition, the presence of genotype–phenotype correlations is controversial in GNE myopathy, with most reports denying significant correlations [7]. In fact, substantial heterogeneity is observed among participants who have the same mutations. For example, few subjects with p.D176V and p.M712T mutations exhibited a normal or very mild phenotype, with disease onset after the age of 60 [3,13]. Furthermore, only a limited number of studies that analyze compound heterozygous patients are available. Nonetheless, such studies report a variable degree of severity [14–17].

To clarify the potential relationship between genotype and clinical phenotype (*i.e.*, age at onset, disease course, and current symptoms) of GNE myopathy, we performed a questionnaire-based survey of participants with confirmed GNE myopathy.

2. Participants and methods

2.1. Study population

We obtained approval for this study from the Medical Ethics Committee of the National Center of Neurology and Psychiatry (NCNP). Seventy-eight participants with known GNE myopathy were seen at 8 hospitals specializing in muscle disorders in Japan and 83 participants (not all genetically diagnosed) from the Participants Association for Distal Myopathies (PADM) were recruited. Participants provided written informed consent prior to completing the questionnaire.

A total of 75 participants completed and returned the questionnaire. Of the 75 participants analyzed, 4 were found to have only one heterozygous mutation. Because single heterozygous mutations have not been confirmed to cause GNE myopathy, these 4 participants were excluded from this study.

2.2. Study design

The present study is a retrospective and cross-sectional analysis, which includes 71 participants with genetically confirmed GNE myopathy. Clinical information was collected from participants using a questionnaire and genetic information was acquired from available medical records.

2.3. Questionnaire

Participants completed a self-reporting questionnaire regarding 1) developmental and past symptoms, 2) past and present ambulatory status, and 3) information about diagnosis and medical services (Supplementary material, original version in Japanese).

To determine developmental history, we collected the following information: 1) trouble before and/or during delivery, 2) body weight and height at birth, 3) age at first gait, 4) exercise performance during nursery, kindergarten, or school, and 5) age at onset and signs of first symptoms. Participants were also asked about the onset of 1) gait disturbance, 2) walking with assistance (*i.e.*, cane and/or orthotics and/or handrails), 3) wheelchair use, 4) loss of ambulation, and 5) current gait performance. With regard to medical history, participants were asked about 1) age at the time of first hospital visit, 2) whether or not they had symptoms at the time of visit, 3) age at the time of final diagnosis, 4) how many hospitals/clinics were visited before final diagnosis, and 5) whether a biopsy was performed.

2.4. Medical record examination

To verify the accuracy of the information provided by each participant, available medical records from 17 participants (23.9%) seen at outpatient clinics at NCNP were examined (9 males and 8 females).

2.5. Data handling and analysis

All variables were summarized using descriptive statistics, which included mean, standard deviation (SD), median, range, frequency, and percentage. Each variable was compared against age, sex, genotype, and domain mutation (*i.e.*, within the UDP-GlcNAc 2-epimerase domain: ED or *N*-acetylmannosamine kinase domain: KD). Student's *t* test was used to compare the means for each participant group (ED/ED, ED/KD and KD/KD participants). Data from the two participant groups were calculated using chi-square contingency table analysis. The time from disease onset to walking with assistance, time from disease onset to wheelchair use, and time from disease onset to loss of ambulation were evaluated using the Kaplan–Meier method with log-rank analysis. Questionnaire reliability was tested using intraclass correlation coefficients (ICCs), and two-sided 95% confidence intervals (CIs) were calculated using a one-way random effects analysis of variance model for inter-rater reliability. All analyses were performed using SPSS for Macintosh (version 18, SPSS Inc., Chicago, IL).

3. Results

3.1. General characteristics

A total of 71 Japanese individuals (27 males and 44 females) participated in the study. The mean age at data collection was 43.1 ± 10.7 years. None of the participants showed developmental abnormalities during infancy or early childhood.

3.2. GNE mutations

Forty-one percent of study participants (n = 29/71) had homozygous mutations, while 59% (n = 42/71) had compound heterozygous mutations (Table 1). Among homozygous participants, 86.2% (n = 25/29) harbored the p.V572L mutation, while the remaining participants had other mutations. No homozygous participants for the p.D176V mutation were identified. Among compound heterozygous participants, 28.5% (n = 12/42) had p.D176V/p.V572L mutations, while the remaining participants had other mutations. With respect to allelic frequency, 50.0% (71/142) were p.V572L, 20.4% (29/142) p.D176V, 3.5% (5/142) p.C13S, 2.8% (4/142) p.M712T, and 2.1% (3/142) p.A630T. All other mutations accounted for 2%. A total of 18.3% (n = 13/71) of participants were homozygous with a mutation in the GNE domain (ED/ED), 39.4% (n = 28/71) of participants were compound heterozygous with a mutation in the GNE domain and one in the MNK domain (ED/KD), and 42.3% (n = 30/71) of participants had a mutation in the MNK domain in both alleles (KD/KD).

3.3. Past and present symptoms

Mean participant age at symptom onset was 25.2 ± 9.2 years (range, 12–58 years; median, 24.5 years). There was no significant difference between males and females for current age, age at disease

Please cite this article as: Mori-Yoshimura M, et al, Heterozygous UDP-GlcNAc 2-epimerase and *N*-acetylmannosamine kinase domain mutations in the *GNE*..., J Neurol Sci (2012), doi:10.1016/j.jns.2012.03.016

Table 1
Genotypes of the GNE myopathy patient population.

		Questionnaire	Outpatients
ED/ED	Total	13	4
	Homozygote	1	0
	p.C13S homozygote	1	
	Compound heterozygote	12	4
	p.C13S/p.M29T	1	1
	p.C13S/p.A631	1	1
	p.D176V/p.F233S	1	1
	p.D176V/p.R306Q	2	
	p.R129Q/p.D176V	1	
	p.R129Q/p.R277C	1	
	p.D27L/p.D176V	1	1
	p.B89S/p.D176V	1	
	p.D176V/p.R246W	1	
	p.D176V/p.R321C	1	
	p.D176V/p.V331A	1	
ED/KD	Total	28	8
	Compound heterozygote	28	8
	p.D176V/p.V572L	12	3
	p.C13S/p.V572L	1	1
	p.D176V/p.I472T	1	1
	p.D176V/p.L603F	1	1
	p.R177C/p.V572L	1	1
	383insT/p.V572L	1	1
	p.D176V/p.G708S	2	
	p.D187G/p.V572L	2	
	p.R8X/p.V572L	1	
	p.D176V/p.G568S	1	
	p.D176V/p.H626R	1	
	p.D176V/p.A630T	1	
	p.I276T/p.V572L	1	
	p.G295D/p.A631V	1	
	p.A600E/p.D176V	1	
KD/KD	Total	30	5
	Homozygote	28	5
	p.V572L homozygote	25	4
	p.M712T homozygote	2	
	p.A630T homozygote	1	
	Compound heterozygote	2	0
	p.V572L/p.R420X	1	1
	1756Gdel (stop)/p.V572L	1	

onset, age at walking with assistance, age at wheelchair use, and current ambulatory status. Initial symptoms included gait disturbance (66.2%, n = 47/71), other lower limb symptoms (26.8%, n = 19/71), easily fatigued (23.9%, n = 17/71), and weakness of hands and fingers (8.5%, n = 6/71). In addition, 21.1% (n = 15/71) had onset of symptoms before the age of 20. When specifically asked, 47.8% (n = 34/71) described themselves as slow runners during childhood, and 42.5% reported having had difficulty with physical exercise during school years.

3.4. Diagnosis

Mean participant age at diagnosis was 33.9 ± 12.6 years (median, 29.5 years; range 17 to 67 years). Mean participant age at first physician visit was 29.6 ± 10.4 years (median, 27 years; range, 12–62 years), and mean time between first visit and diagnosis was 4.4 ± 8.3 years.

3.5. Walking with assistance and wheelchair use

At the time of the survey, 52.0% (n = 37/71) were ambulant (41.3 ± 12.8 years); however, only 15.5% (n = 11/71, 40.0 ± 13.6 years) could walk without assistance, with the remaining 35.2% requiring assistance (n = 25/71, 41.8 ± 12.7 years). Only 7.0% of these participants (n = 5/71) could walk up stairs, while 49.3% (n = 35/71) were non-ambulant. Wheelchairs were used by 63.6% (23.9% partially bound and 43.7% totally bound) and an electric wheelchair was used by 41.9% (n = 31/71). Mean participant age of wheelchair users was 34.9 ± 11.7 years (range, 18–70 years). Wheelchairs were not used by 32.4% (n = 26/71) of participants. Current age of wheelchair-free participants was 39.4 ± 12.3 years (range, 21–61 years; median, 34 years) and that of wheelchair-bound participants was 42.8 ± 12.6 years (range, 21–71; median, 42 years).

Kaplan–Meier analysis revealed a median proportional age at walking with assistance of 30.0 ± 1.4 years. Median proportional age of wheelchair users was 36.0 ± 2.7 years, and that for loss of ambulation was 45.0 ± 4.2 years. The time from disease onset to walking with assistance was 7.0 ± 0.4 years, time from disease onset to wheelchair use was 11.5 ± 1.2 years, and time from disease onset to loss of ambulation was 17.0 ± 2.1 years.

3.6. Correlation between disease genotype and phenotype

To determine if a correlation between genotype and phenotype existed, we compared domain mutations (ED/KD, or both) available from medical reports to questionnaire answers (Table 2). Participants with KD/KD mutations (both homozygous and heterozygous) were younger and more severely affected compared to participants with ED/KD or ED/ED mutations. No significant difference in current age or age at disease onset between ED/ED and ED/KD participants was identified. Kaplan–Meier analyses revealed that the proportional time from disease onset to wheelchair use and from disease onset to loss of ambulation was significantly shorter in KD/KD compared to ED/KD participants. ED/ED participants exhibited a shorter time of disease onset to wheelchair use compared to ED/KD participants (Table 3, Fig. 1).

3.7. Comparison between p.V572L homozygous and p.D176V/p.V572L compound heterozygous participants

To compare clinical features in patients with the same mutations, we specifically analyzed data from those with p.V572L (n = 25/71, 35.2%) and p.D176V/p.V572L (n = 12/71, 16.9%) mutations, as these two were the most frequent mutations in our study population (Table 2). Age at disease onset of homozygous participants (p.V572L) was 21.3 ± 5.7 years (range, 12–32 years) and time from disease onset to wheelchair use was 11.3 ± 5.4 years (range, 3–21 years). Only 16.0% (n = 4/25) of these homozygous participants reported that they were not currently using a wheelchair. In contrast, the mean age at disease onset of heterozygous participants (p.D176V/p.V572L) was 35.5 ± 14.1 years (range, 13.5–57 years) and time from disease onset to wheelchair use was 17.9 ± 7.0 years (range, 11–28 years). A total of 66.7% of these compound heterozygous participants (n = 8/12) reported that they were not using a wheelchair.

3.8. Questionnaire response compared to medical records

Questionnaires from 17 participants (NCNP outpatient participants) were compared to available medical records (Table 2). Age at disease onset, age at onset of gait disturbance, age at walking with assistance, and age at loss of ambulation were assessed for inter-rater reliability. Age at disease onset, age at onset of gait disturbance, age at walking with assistance, and age at loss of ambulation were assessed for inter-rater reliability. ICC values were 0.979 (95% CI 0.941–0.992) for age at disease onset, 0.917 (95% CI 0.752–0.972) for age at onset of gait disturbances, 0.985 (95% CI 0.949–0.995) for age at walking with assistance, and 0.967 (95% CI 0.855–0.993) for age at loss of ambulation.

4. Discussion

The present study provides a detailed overview of disease severity and progression in 71 Japanese participants with genetically confirmed GNE myopathy. Questionnaire-based surveys have been used to study

Please cite this article as: Mori-Yoshimura M, et al, Heterozygous UDP-GlcNAc 2-epimerase and *N*-acetylmannosamine kinase domain mutations in the *GNE*..., J Neurol Sci (2012), doi:10.1016/j.jns.2012.03.016

Table 2
Comparison of disease course among genotypes.

		Total	ED/ED	ED/LD	KD/KD
Questionnaire	*n*	71	13	28	30
	Age (years old)	43.1 ± 10.7	44.2 ± 11.2	45.3 ± 13.4	40.6 ± 13.0
	Age at onset (years old)	25.5 ± 9.2	26.3 ± 7.3^{+}	29.8 ± 11.0*	21.2 ± 5.5$^{*,+}$
	Age at walking with assistance	31.8 ± 10.0	34.0 ± 11.1	35.6 ± 10.9*	27.8 ± 6.8*
	Duration from onset to walking with assistance	8.4 ± 6.5	7.5 ± 7.3	9.2 ± 6.5	8.0 ± 6.6
	Wheelchair user (%)	48 (67.8)	10(76.9)	14 (50.0)*	24 (80.0)*
	Wheelchair use since (age)	37.6 ± 8.6	36.4 ± 12.0	43.0 ± 8.7*	31.2 ± 9.3*
	Number of patients with lost ambulation	35 (49.8)	6(46.2)	8 (28.6)*	21 (70.0)*
	Age at lost ambulation	33.6 ± 9.2	31.2 ± 6.0	39.7 ± 9.5	32.1 ± 9.3
	Duration from onset to loss of ambulation	12.2 ± 5.2	9.8 ± 3.5	13.8 ± 6.4	12.4 ± 5.1
NCNP outpatients	*n*	17	4	8	5
	Age (years old)	43.9 ± 14.1	53.5 ± 8.9^{+}	44.3 ± 16.3	35.6 ± 9.2^{+}
	Age at onset (years old)	25.8 ± 9.2	33.4 ± 9.2^{+}	29.6 ± 13.5	19.6 ± 4.2^{+}
	Duration from onset to walking with assistance	7.5 ± 4.2	8.9 ± 5.1	8.1 ± 4.7	5.2 ± 1.5
	Wheelchair user (%)	12 (70.6)	3 (75.0)	4 (50.0)	4 (100)
	Wheelchair use since (age)	33.3 ± 12.6	47.5 ± 17.7	35.2 ± 12.4	25.8 ± 6.3
	Number of patients with lost ambulation	9 (52.9)	3 (75.0)	3 (28.6)*	5 (100)*
	Age at lost ambulation	33.8 ± 9.3	40.0 ± 0.0	39.0 ± 16.5	31.0 ± 8.2
	Duration from onset to loss of ambulation	10.7 ± 4.2	11.2 ± 5.6	11.1 ± 7.8	6.2 ± 2.6

In the questionnaire group, age at onset and age at walking with assistance were significantly younger in KD/KD patients than in ED/KD patients. The number of wheelchair users and patients with loss of ambulation was significantly higher in the KD/KD group than in the ED/KD group. In contrast, with the exception of age at onset, there were no significant differences between ED/ED and ED/KD or KD/KD patients in these clinical parameters. The ED/ED patients were older than the others, and KD/KD patients tended to show the fastest progression.

* $p<0.05$ between ED/KD and KD/KD.

$^{+}$ $p<0.05$ between ED/ED and KD/KD.

the natural disease course of other rare neuromuscular disorders, such as Pompe disease [18] and spinal muscular atrophy type-1 [19]. It is difficult to establish the natural history of such rare disorders using medical records only because patients are typically seen in many different hospitals. In the present study, we used a self-reporting questionnaire and support its use for complementing medical records because it provides a more complete disease overview and establishes specific clinical trends or correlations. Indeed, our questionnaire demonstrates excellent inter-rater reliability against medical records and yields several findings regarding differences in disease progression among genetically distinct, GNE myopathy participants.

Only 15.5% of participants could walk and 7.0% could walk up stairs without assistance, which reflects the fact that GNE myopathy patients often require canes and/or leg braces at an early disease stage. This indicates that traditional six-minute walk or four-step walking tests often used to evaluate muscular dystrophies or myopathies can only be applied in a very limited number of cases, such as natural disease course studies or clinical trials. Therefore, alternate evaluation tools are required, which should include functional measurements that can be completed without canes or braces. For example, the Gross Motor Function Measure is a useful tool for evaluating mildly and severely affected patients [20].

The male to female ratio in our study population (27 males and 44 females) was skewed from the expected ratio for autosomal recessive inheritance. However, the male to female ratio of the 17 NCNP outpatient participants was 9:8. One possible explanation for the observed sex ratio in our study population is that female participants tend to be more enthusiastic toward questionnaire-based and/or PADM activities. There was no significant difference in age at survey and age at disease onset between male and female participants. However, in a mouse model of GNE myopathy, weight loss and muscle atrophy were more pronounced and occurred earlier in females compared to males [11].

We showed that KD/KD mutations are associated with a more severe phenotype compared to ED/KD mutations. Indeed, KD/KD participants had an earlier disease onset, a more rapid and progressive disease course, and a shorter time from disease onset to loss of ambulation. This was also observed in the 17 NCNP outpatient participants analyzed in our study. In contrast, ED/ED participants did not show significant differences across disease course parameters analyzed except for an earlier and later age at disease onset compared to ED/KD and KD/KD participants, respectively. Thus, ED/ED participants appear to have a disease severity intermediate between ED/KD and KD/KD participants. One possible explanation is that the major mutation, p.V572L, may be associated with a more severe phenotype. In general, the reasons for this earlier onset and disease progression remain unknown. Jewish GNE myopathy patients with homozygous p.M712T mutations have a milder phenotype compared to Japanese patients, as most of their quadriceps are spared and they usually become wheelchair-bound 15 years or more after disease onset [13,21]. Our study population included two women with homozygous p.M712T mutations: a 38 year-old ambulant and a 35 year-old non-ambulant participant. Although the two participants had a slightly later disease onset (ages 23 and 27 years, respectively) compared to KD/KD participants, the difference was not significant.

An asymptomatic patient with a p.D176V homozygous mutation was previously reported [3]. The study suggested that p.D176V homozygous patients may show a mild or late disease onset phenotype. The results presented here may support this observation as no p.D176V homozygous participants were present in our study

Table 3
Inter-rater reliability of the questionnaire.

	Onset	Age of gait disturbance	Age of gait with help	Age at loss of ambulant
Number of patients	17	17	13	9
ICC (95% CI)	0.979 (0.941–0.992)	0.917 (0.752–0.972)	0.985 (0.949–0.995)	0.967 (0.855–0.993)
p	0.000	0.000	0.000	0.000

Age at onset, age at onset of gait disturbances, age at walking with assistance, and age at loss of ambulation were assessed in a subgroup of 17 outpatients to evaluate the inter-rater reliability of the questionnaire.

Please cite this article as: Mori-Yoshimura M, et al, Heterozygous UDP-GlcNAc 2-epimerase and *N*-acetylmannosamine kinase domain mutations in the *GNE*..., J Neurol Sci (2012), doi:10.1016/j.jns.2012.03.016

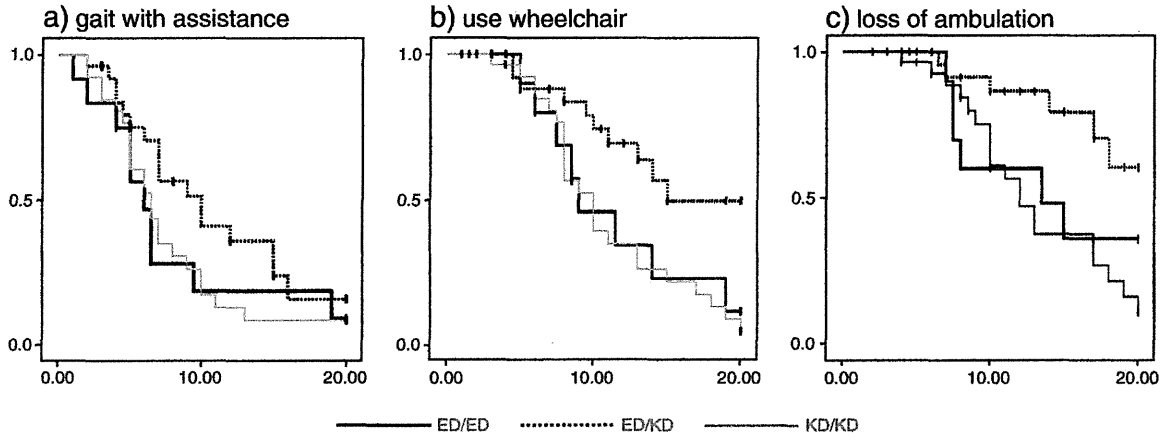

Fig. 1. Kaplan–Meier analysis of time from disease onset to (a) walking with assistance, (b) wheelchair use, and (c) loss of ambulation. Significant differences between ED/KD and KD/KD genotypes were identified. Age at disease onset was significantly different between ED/ED participants and ED/KD and KD/KD participants.

population, although p.D176V was the second most common mutation carried by 29 of our participants. In addition, a high variability was observed regarding age at disease onset and disease progression, underscoring the role of a yet-to-be identified factor(s) in determining disease phenotype.

The recruitment of participants from PADM and highly specialized neurology hospitals is a potential source of selection bias and thus a limitation of this study. These participants are likely to be more motivated because they are more severely affected compared to the general patient population. Furthermore, patients with lower disease severity may not yet be diagnosed with GNE myopathy. Therefore, our study may not accurately reflect the general patient population. Nevertheless, we believe our findings provide important information as our study population covers a broad range in age (22 to 81 years) and symptoms (minimal to wheelchair-bound). Finally, recall bias may also affect results presented in this retrospective study. Therefore, future studies should be performed with an emphasized prospective design.

In conclusion, our study shows that the KD/KD genotype (*i.e.*, p.V572L homozygous mutation) is associated with a more severe phenotype compared to compound heterozygous ED/KD mutations. Because only a small number of participants could walk, future studies should include ambulation-independent motor tests to yield a more comprehensive clinical overview in GNE myopathy patients with different genotypes.

Supplementary data to this article can be found online at doi:10.1016/j.jns.2012.03.016.

Conflict of interest

We certify that there is no conflict of interest with any financial organization regarding the material discussed in the manuscript.

Acknowledgments

We thank members of the Patients Association for Distal Myopathies (PADM) for their help. This work was partly supported by the Research on Intractable Diseases of Health and Labor Sciences Research Grants; Comprehensive Research on Disability Health and Welfare Grants, Health and Labor Science Research Grants; Intramural Research Grant (23-4, 23-5) for Neurological and Psychiatric Disorders of NCNP; and a Young Investigator Fellowship from the Translational Medical Center, NCNP.

References

[1] Nonaka I, Sunohara N, Satoyoshi E, Terasawa K, Yonemoto K. Autosomal recessive distal muscular dystrophy: a comparative study with distal myopathy with rimmed vacuole formation. Ann Neurol 1985;17:51–9.
[2] Argov Z, Yarom R. "Rimmed vacuole myopathy" sparing the quadriceps. A unique disorder in Iranian Jews. J Neurol Sci 1984;64:33–43.
[3] Nishino I, Noguchi S, Murayama K, Driss A, Sugie K, Oya Y, et al. Distal myopathy with rimmed vacuoles is allelic to hereditary inclusion body myopathy. Neurology 2002;59:1689–93.
[4] Eisenberg I, Avidan N, Potikha T, Hochner H, Chen M, Olender T, et al. The UDP-N-acetylglucosamine 2-epimerase/N-acetylmannosamine kinase gene is mutated in recessive hereditary inclusion body myopathy. Nat Genet 2001;29:83–7.
[5] Kayashima T, Matsuo H, Satoh A, Ohta T, Yoshiura K, Matsumoto N, et al. Nonaka myopathy is caused by mutations in the UDP-N-acetylglucosamine-2-epimerase/N-acetylmannosamine kinase gene (GNE). J Hum Genet 2002;47:77–9.
[6] Keppler OT, Hinderlich S, Langner J, Schwartz-Albiez R, Reutter W, Pawlita M. UDP-GlcNAc 2-epimerase: a regulator of cell surface sialylation. Science 1999;284:1372–6.
[7] Malicdan MC, Noguchi S, Nishino I. Recent advances in distal myopathy with rimmed vacuoles (DMRV) or hIBM: treatment perspectives. Curr Opin Neurol 2008;21:596–600.
[8] Noguchi S, Keira Y, Murayama K, Ogawa M, Fujita M, Kawahara G, et al. Reduction of UDP-N-acetylglucosamine 2-epimerase/N-acetylmannosamine kinase activity and sialylation in distal myopathy with rimmed vacuoles. J Biol Chem 2004;279:11402–7.
[9] Broccolini A, Gidaro T, De Cristofaro R, Morosetti R, Gliubizzi C, Ricci E, et al. Hyposialylation of neprilysin possibly affects its expression and enzymatic activity in hereditary inclusion–body myopathy muscle. J Neurochem 2008;105:971–81.
[10] Salama I, Hinderlich S, Shlomai Z, Eisenberg I, Krause S, Yarema K, et al. No overall hyposialylation in hereditary inclusion body myopathy myoblasts carrying the homozygous M712T GNE mutation. Biochem Biophys Res Commun 2005;328:221–6.
[11] Malicdan MC, Noguchi S, Nonaka I, Hayashi YK, Nishino I. A Gne knockout mouse expressing human GNE D176V mutation develops features similar to distal myopathy with rimmed vacuoles or hereditary inclusion body myopathy. Hum Mol Genet 2007;16:2669–82.
[12] Malicdan MC, Noguchi S, Hayashi YK, Nonaka I, Nishino I. Prophylactic treatment with sialic acid metabolites precludes the development of the myopathic phenotype in the GNE myopathy mouse model. Nat Med 2009;15:690–5.
[13] Argov Z, Eisenberg I, Grabov-Nardini G, Sadeh M, Wirguin I, Soffer D, et al. Hereditary inclusion body myopathy: the Middle Eastern genetic cluster. Neurology 2003;60:1519–23.
[14] Tomimitsu H, Shimizu J, Ishikawa K, Ohkoshi N, Kanazawa I, Mizusawa H. Distal myopathy with rimmed vacuoles (DMRV): new GNE mutations and splice variant. Neurology 2004;11:1607–10.
[15] Yabe I, Higashi T, Kikuchi S, Sasaki H, Fukazawa T, Yoshida K, et al. GNE mutations causing distal myopathy with rimmed vacuoles with inflammation. Neurology 2003;12:384–6.
[16] Chu CC, Kuo HC, Yeh TH, Ro LS, Chen SR, Huang CC. Heterozygous mutations affecting the epimerase domain of the GNE gene causing distal myopathy with rimmed vacuoles in a Taiwanese family. Clin Neurol Neurosurg 2007;109:250–6.
[17] Ro LS, Lee-Chen GJ, Wu YR, Lee M, Hsu PY, Chen CM. Phenotypic variability in a Chinese family with rimmed vacuolar distal myopathy. J Neurol Neurosurg Psychiatry 2005;76:752–5.

Please cite this article as: Mori-Yoshimura M, et al. Heterozygous UDP-GlcNAc 2-epimerase and *N*-acetylmannosamine kinase domain mutations in the *GNE*..., J Neurol Sci (2012), doi:10.1016/j.jns.2012.03.016

[18] Hagemans ML, Winkel LP, Van Doorn PA, Loonen MC, Hop WJ, Reuser AJ, et al. Clinical manifestation and natural course of late-onset Pompe's disease in 54 Dutch patients. Brain 2005;128:671–7.
[19] Oskoui M, Levy G, Garland CJ, Gray JM, O'Hagen J, De Vivo DC, et al. The changing natural history of spinal muscular atrophy type 1. Neurology 2007;69: 1931–6.
[20] Sienko Thomas S, Buckon CE, Nicorici A, Bagley A, McDonald CM, Sussman MD. Classification of the gait patterns of boys with Duchenne muscular dystrophy and their relationship to function. J Child Neurol 2010;25:1103–9.
[21] Eisenberg I, Grabov-Nardini G, Hochner H, Korner M, Sadeh M, Bertorini T, et al. Mutations spectrum of GNE in hereditary inclusion body myopathy sparing the quadriceps. Hum Mutat 2003;21:99.

Please cite this article as: Mori-Yoshimura M, et al, Heterozygous UDP-GlcNAc 2-epimerase and *N*-acetylmannosamine kinase domain mutations in the *GNE*..., J Neurol Sci (2012), doi:10.1016/j.jns.2012.03.016

Journal of Human Genetics (2013), 1–8

www.nature.com/jhg

ORIGINAL ARTICLE

Exome sequencing identifies a novel *TTN* mutation in a family with hereditary myopathy with early respiratory failure

Rumiko Izumi[1,2], Tetsuya Niihori[1], Yoko Aoki[1], Naoki Suzuki[2], Masaaki Kato[2], Hitoshi Warita[2], Toshiaki Takahashi[3], Maki Tateyama[2], Takeshi Nagashima[4], Ryo Funayama[4], Koji Abe[5], Keiko Nakayama[4], Masashi Aoki[2] and Yoichi Matsubara[1]

Myofibrillar myopathy (MFM) is a group of chronic muscular disorders that show the focal dissolution of myofibrils and accumulation of degradation products. The major genetic basis of MFMs is unknown. In 1993, our group reported a Japanese family with dominantly inherited cytoplasmic body myopathy, which is now included in MFM, characterized by late-onset chronic progressive distal muscle weakness and early respiratory failure. In this study, we performed linkage analysis and exome sequencing on these patients and identified a novel c.90263G>T mutation in the *TTN* gene (NM_001256850). During the course of our study, another groups reported three mutations in *TTN* in patients with hereditary myopathy with early respiratory failure (HMERF, MIM #603689), which is characterized by overlapping pathologic findings with MFMs. Our patients were clinically compatible with HMERF. The mutation identified in this study and the three mutations in patients with HMERF were located on the A-band domain of titin, suggesting a strong relationship between mutations in the A-band domain of titin and HMERF. Mutation screening of *TTN* has been rarely carried out because of its huge size, consisting of 363 exons. It is possible that focused analysis of *TTN* may detect more mutations in patients with MFMs, especially in those with early respiratory failure.
Journal of Human Genetics advance online publication, 28 February 2013; doi:10.1038/jhg.2013.9

Keywords: A-band; cytoplasmic body; Fn3 domain; hereditary myopathy with early respiratory failure; HMERF; myofibrillar myopathy; titin; *TTN*

INTRODUCTION

Myofibrillar myopathies (MFMs) were proposed in 1996 as a group of chronic muscular disorders characterized by common morphologic features observed on muscle histology, which showed the focal dissolution of myofibrils followed by the accumulation of products of the degradative process.[1] The clinical phenotype of MFM is characterized by slowly progressive muscle weakness that can involve proximal or distal muscles, with onset in adulthood in most cases. However, other phenotypes are highly variable. Although 20% of patients with MFMs have been revealed to have mutations in *DES*, *CRYAB*, *MYOT*, *LDB* (*ZASP*), *FLNC* or *BAG3*, the major genetic basis of MFMs remains to be elucidated.

Respiratory weakness is one of the symptoms of MFMs. The early or initial presentation of respiratory failure is not a common manifestation of MFMs as a whole, and there are limited reports regarding a fraction of patients with *DES*,[2] *MYOT*[3] or *CRYAB*[4] mutation. In 1993, our group reported a Japanese family with dominantly inherited cytoplasmic body (CB) myopathy,[5] which is now included in MFM. Currently, this family includes 20 patients in five successive generations who show almost homogeneous clinical features characterized by chronic progressive distal muscle weakness and early respiratory failure. However, the underlying genetic etiology in this family was unknown. The aim of this study was to determine the genetic cause in this family. To identify the responsible genetic mutation, we performed linkage analysis and whole-exome sequencing.

MATERIALS AND METHODS

This study was approved by the Ethics Committee of the Tohoku University School of Medicine, and all individuals gave their informed consent before their inclusion in the study.

[1]Department of Medical Genetics, Tohoku University School of Medicine, Sendai, Japan; [2]Department of Neurology, Tohoku University School of Medicine, Sendai, Japan; [3]Department of Neurology and Division of Clinical Research, National Hospital Organization Nishitaga National Hospital, Sendai, Japan; [4]Division of Cell Proliferation, United Centers for Advanced Research and Translational Medicine, Tohoku University Graduate School of Medicine, Sendai, Japan and [5]Department of Neurology, Okayama University Medical School, Okayama, Japan
Correspondence: Dr Y Aoki, Department of Medical Genetics, Tohoku University School of Medicine, 1-1 Seiryo-machi, Aoba-ku, Sendai 980-8574, Japan.
E-mail: aokiy@med.tohoku.ac.jp
or Professor M Aoki, Department of Neurology, Tohoku University School of Medicine, 1-1 Seiryo-machi, Aoba-ku, Sendai 980-8574, Japan.
E-mail: aokim@med.tohoku.ac.jp
Received 23 October 2012; revised 9 January 2013; accepted 10 January 2013

Clinical information on the family

This family includes 20 patients (13 males and 7 females) in five successive generations (Figure 1). The family is of Japanese ancestry, and no consanguineous or international mating was found. Of all patients, seven underwent a muscle biopsy, and two were autopsied. All of the histological findings were compatible with MFM (see clinical data).

The age of onset ranged from 27–45 years. The most common presenting symptom was foot drop. At the initial evaluations, muscle weakness was primarily distributed in the ankle dorsiflexors and finger extensors. The patients were generally built and showed no other extramuscular abnormalities. In addition to this chronic progressive distal muscle weakness, respiratory distress occurred between 0 and 7 years from the initial onset (average 3.8 years) in seven patients (IV-9, V-2, A, B, E, H, and J) with adequate clinical information. Two patients who had not had any respiratory care died of respiratory failure approximately a decade from the initial onset. The other patients have been alive for more than 10 years (maximum 18 years) but require nocturnal non-invasive positive pressure ventilation. They were 37–58 years of age as of 2012 and able to walk independently with or without a simple walking aid. Although the time at which patients recognized dysphagia or dysarthria varied between 1 to more than 10 years from the initial onset, decreased bulbar functions had been noted at the initial evaluation in most cases. Cardiac function was normally maintained in all patients of the family.

Clinical data

The level of serum creatine kinase was normal or mildly elevated. Electromyography of affected muscles showed a chronic myogenic pattern, and the nerve conduction study did not suggest any neuropathic involvement. Muscle imaging showed focal atrophy in the tibialis anterior, tibialis posterior, extensor hallucis and digitorum longus, peroneal and semitendinosus muscle on initial assessment (Figure 2A), and atrophy became clear in cervical muscles, shoulder girdles, intercostals and proximal limb muscles in the following several years. Upon muscle biopsy, the most common finding was numerous cytoplasmic bodies (CBs), which were found on 7.3% of myofibers in the tibialis anterior of individual E (Figure 2B (a–c)) and 50–80% of intercostals in other cases.[5] Other nonspecific findings were increased variability in the size of myofibers, central nuclei and rimmed vacuoles observed on a few fibers. No strong immunoreaction of desmin was seen in the CBs (Figure 2B (d, e)). An electron microscope examination showed that the regular sarcoplasmic pattern was replaced by abnormal fine filamentous structures, which seemed to attach to the Z-band. CBs were also found in almost all skeletal muscles and some smooth muscles in autopsied cases.[5] Cardiac myofibers also contained numerous CBs in one of the autopsied cases (V-2),[5] although the patient did not present any cardiac complication. The sequence analysis of the coding regions and flanking introns of *DES* and *MYOT* showed no pathogenic mutation in individual E. An array comparative genomic hybridization performed with the Agilent SurePrint G3 Human CGH 1M microarray format in individual A did not reveal any aberrations of genomic copy number.

Linkage analysis

DNA was extracted by standard methods. Linkage analysis was performed on nine family members (A–I in Figure 1; four of them were affected, and the others were unaffected) through genotyping using an Illumina Human Omni 2.5 BeadChip (Illumina, San Diego, CA, USA). We chose single-nucleotide polymorphisms (SNPs) that satisfied all of the following criteria: (1) autosomal SNPs whose allele frequencies were available from the HapMap project (http://hapmap.ncbi.nlm.nih.gov/), (2) SNPs that were not monomorphic among members and (3) SNPs that were not in strong linkage disequilibrium with neighboring SNPs (r2 values <0.9). Then, we selected the first five SNPs from each position of integer genetic distance from SNPs that met the above criteria for the initial analysis. The details were as follows; we chose a SNP closest to 0 cM and the neighboring four SNPs. If the genetic distance of a SNP was the same as that of the next SNP, we considered the genomic position to determine their order. We repeated this process at 1 cM, 2 cM and so on.

We performed a multipoint linkage analysis of the data set (17 613 SNPs) using MERLIN[6] 1.1.2 under the autosomal dominant mode with the following parameters: 0.0001 for disease allele frequency, 1.00 for individuals heterozygous and homozygous for the disease allele and 0.00 for individuals

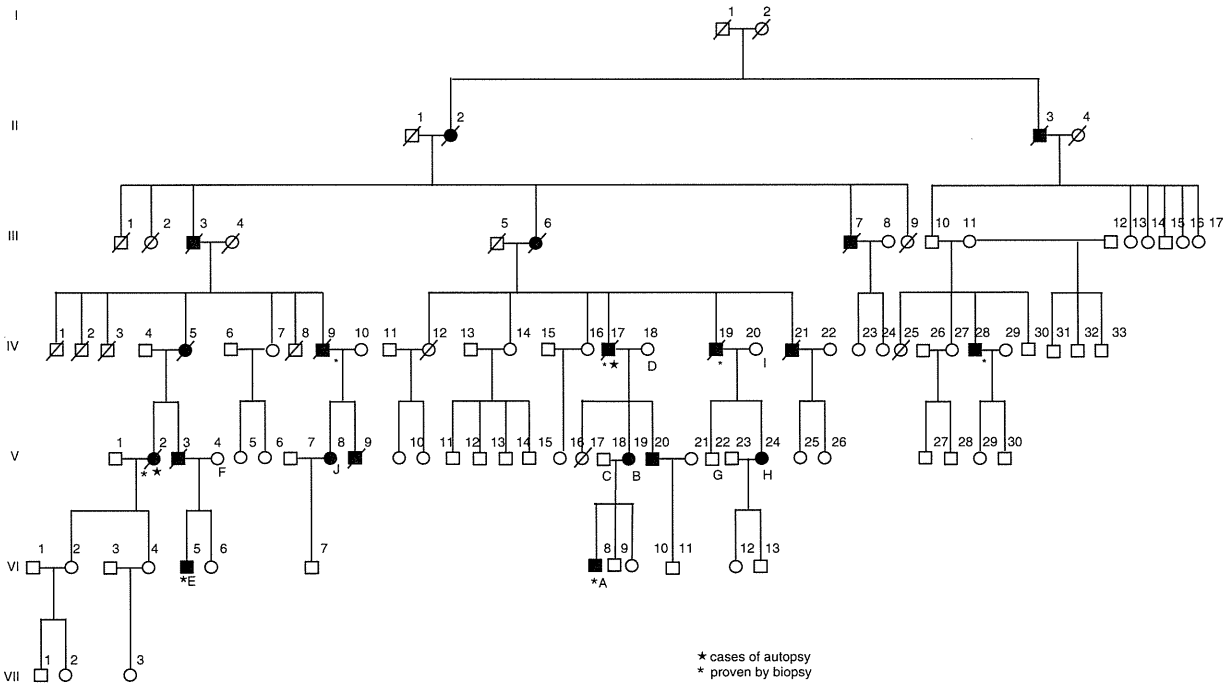

Figure 1 Family pedigree. Filled-in symbols indicate individuals with MFM. Empty symbols indicate unaffected individuals. A star and asterisk indicate autopsy-proven and muscle biopsy-proven cases, respectively. (A–J) indicates individuals whose DNA was used for this study.

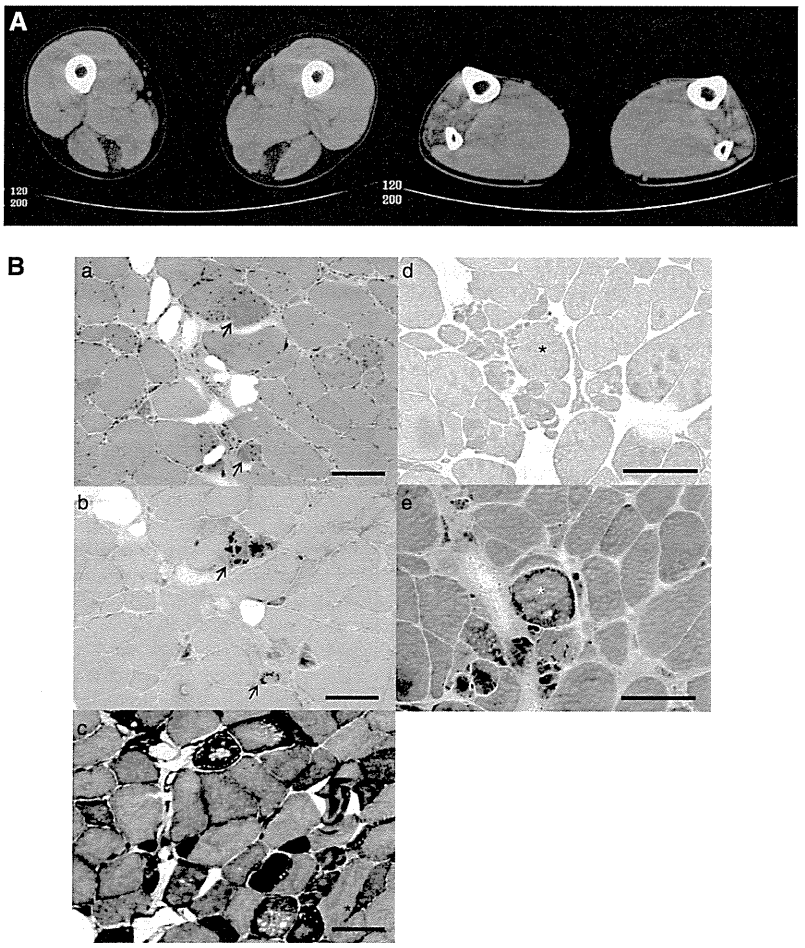

Figure 2 Family clinical data. (**A**) Muscle computed tomography of affected lower extremity. The imaging in the initial assessment of individual A showed symmetrical atrophy and fatty replacement of the semitendinosus in the proximal lower extremities (left) and the tibialis anterior, tibialis posterior, extensor hallucis and digitorum longus, and peroneal muscle in the distal (right) lower extremities. (**B**) Pathology of muscle biopsy. Hematoxylin-eosin (a), Gomori-trichrome (b) and NADH (nicotinamide adenine dinucleotide)-tetrazolium reductase (c) staining of the muscle biopsy sample from the tibialis anterior of individual E are shown. CBs are indicated by arrows. CBs were round or oval, 5–10 μm in diameter and predominantly located in the periphery of type 1 fibers, which stained eosinophilic with hematoxylin-eosin and blue–purple with Gomori-trichrome. NADH-tetrazolium reductase staining showed disorganization of the myofibrillar network. Immunostaining for desmin (d) and Gomori-trichrome staining (e) are serial sections of the muscle biopsy from individual E. Stars indicate corresponding fibers. No strong immunoreaction of desmin was seen in the CBs. Scale bars = 100 μm

homozygous for the alternative allele. After this first analysis, a second analysis was performed with all SNPs fulfilling the above criteria around the peaks identified in the first analysis.

Exome sequencing

Exome sequencing was performed on seven family members in three generations (A–E, H and I in Figure 1), four of whom were affected. Exon capture was performed with the SureSelect Human All Exon kit v2 (individuals E, H and I) or v4 (A–D) (Agilent Technologies, Santa Clara, CA, USA). Exon libraries were sequenced with the Illumina Hiseq 2000 platform according to the manufacturer's instructions (Illumina). Paired 101-base pair reads were aligned to the reference human genome (UCSChg19) using the Burrows-Wheeler Alignment tool.[7] Likely PCR duplicates were removed with the Picard program (http://picard.sourceforge.net/). Single-nucleotide variants and indels were identified using the Genome Analysis Tool Kit (GATK) v1.5 software.[8] SNVs and indels were annotated against the RefSeq database and dbSNP135 with the ANNOVAR program.[9] We used the PolyPhen2 polymorphism phenotyping software tool[10] to predict the functional effects of mutations.

Sanger sequencing

To confirm that mutations identified by exome sequencing segregated with the disease, we performed direct sequencing. PCR was performed with the primers shown in Supplementary Table 1. PCR products were purified with a MultiScreen PCR plate (Millipore, Billerica, MA, USA) and sequenced using BigDye terminator v1.1 and a 3500xL genetic analyzer (Applied Biosystems, Carlsbad, CA, USA).

RESULTS

Linkage analysis

The first linkage analysis identified five regions across autosomes with a logarithm of odds (LOD) score greater than 2 (Figure 3). Of the five regions, two were on chromosome 2 (from 167 cM to 168 cM, with a maximum LOD score of 2.46 and from 182 cM to 185 cM, with a maximum LOD score of 2.71), the other two were on chromosome 8 (from 27 cM to 34 cM, with a maximum LOD score of 2.71 and at 61 cM, with a maximum LOD score of 2.03), and one was on

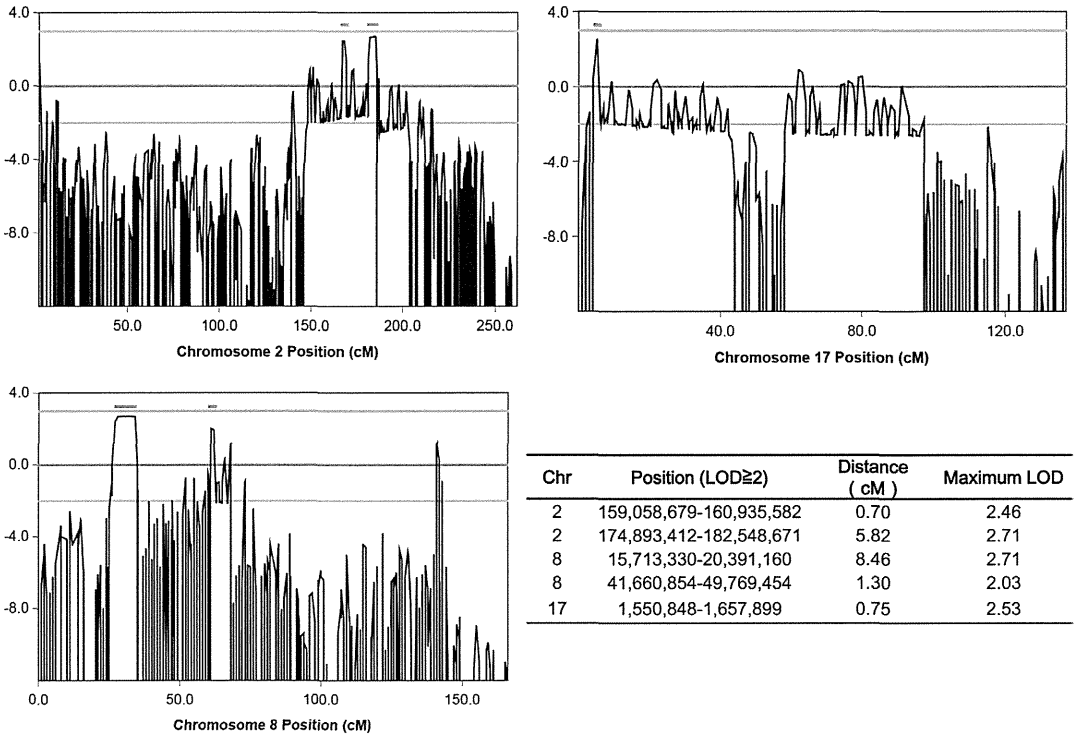

Chr	Position (LOD≧2)	Distance (cM)	Maximum LOD
2	159,058,679-160,935,582	0.70	2.46
2	174,893,412-182,548,671	5.82	2.71
8	15,713,330-20,391,160	8.46	2.71
8	41,660,854-49,769,454	1.30	2.03
17	1,550,848-1,657,899	0.75	2.53

Figure 3 Linkage analysis. Linkage analysis was performed on nine family members (four of them were affected, the others were unaffected) using an Illumina Human Omni 2.5 BeadChip. Five regions with an LOD score greater than 2 (indicated by bar) were identified. A full color version of this figure is available at the *Journal of Human Genetics* journal online.

Table 1 Summary of detected variants by exome sequencing

Individual *Morbidity*	*A* *Affected*	*B* *Affected*	*C* *Unaffected*	*D* *Unaffected*	*E* *Affected*	*H* *Affected*	*I* *Unaffected*	*Segregated in seven family members*
Exonic, splicing	10089	10064	10079	10065	10230	10194	10216	64
Nonsynonymous, splicing, indel, nonsense	4987	5020	5055	5038	5143	5234	5200	32
Allele frequency not available	577	600	536	555	671	794	786	2

chromosome 17 (at 5 cM, with a maximum LOD score of 2.53). In the second detailed linkage analysis, these peaks were determined to range from 167.49 cM at rs4233674 at position 159 058 679 to 168.19 cM at rs7598162 at position 160 935 582, and from 181.23 cM at rs4402725 at position 174 893 412 to 187.05 cM at rs7420169 at position 182 548 671 on chromosome 2; from 26.42 cM at rs2736043 at position 15 713 330 to 34.88 cM at rs9325871 at position 20 391 160, and from 61.02 cM at rs6999814 at position 41 660 854 to 62.32 cM at rs10957281 at position 49 769 454 on chromosome 8; and from 4.7 cM at rs11078552 at position 1 550 848 to 5.45 cM at rs1057355 at position 1 657 899 on chromosome 17. Haplotypes shared by affected individuals in these regions were confirmed by visual inspection. There were a few incompatible SNPs in these regions, presumably due to genotyping error.

Exome sequencing and segregation analysis

In exome sequencing, an average of 215 million reads enriched by SureSelect v4 (SSv4) and 319 million reads enriched by SureSelect v2 (SSv2) were generated, and 99% of reads were mapped to the reference genome by Burrows-Wheeler Alignment tool. An average of 57% (SSv4) and 61% (SSv2) of those reads were duplicated and removed, and an average of 80% (SSv4) and 66% (SSv2) of mapped reads without duplicates were in target regions. The average coverage of each exome was 163-fold (SSv4) and 130-fold (SSv2). An average of 85% (SSv4) and 69% (SSv2) of target regions were covered at least 50-fold (Supplementary Table 2). On average, 10 133 SNVs or indels, which are located within coding exons or splice sites, were identified per individual (Table 1). A total of 64 variants were common among patients and not present in unaffected individuals, and 32 of those were left after excluding synonymous SNVs. In these variants, only the heterozygous mutation c.90263G>T (NM_001256850) at position 179 410 777 of chromosome 2, which was predicted to p.W30088L in *TTN*, was novel (that is, not present in dbSNP v135 or 1000 genomes). Polyphen2 predicted this mutation as probably damaging. This mutation was located in a candidate region suggested by the linkage analysis in the present study. The other variants were registered with dbSNP135, and the allele frequencies, except for one SNV, rs138183879, in *IKBKB*, ranged from 0.0023 to 0.62.

a

Gene	Chr	Position	Variant type	Reference	Variant	dbSNP v135	Coding change	Prediction	Segregaion analysis
TTN	2	179 410777	Missense	G	T	Not present	W30088L	Probably damaging	Segregating
IKBKB	8	42 188 457	Missense	C	T	rs138183879	T742M	Benign	Non-segregating

b

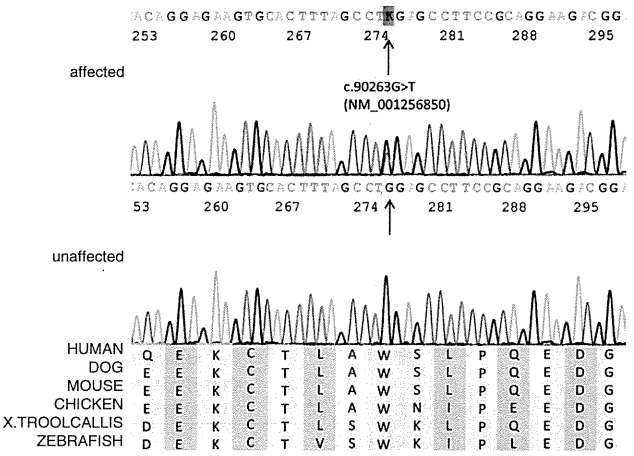

Figure 4 Identified mutations by exome sequencing. (**a**) We performed segregation analysis of two candidates. (**b**) The identified *TTN* mutation and its conservation among species. Sanger sequencing confirmed the heterozygous G to T substitution (indicated by the arrow) at the position chr2;179 410 777, which corresponds to c.90263G>T in exon 293 (NM_001256850.1). The substitution leads to p.W30088L (NP_001243779.1), and this amino acid is conserved among species.

These values were not compatible with the assumption that MFM was a rare disease and showed complete penetrance in this family. The allele frequency of rs138183879 was not available in dbSNP135, and this SNV was in the candidate region on chromosome 8 based on linkage analysis.

We then performed a segregation analysis on the two candidates, the novel mutation c.90263G>T in *TTN* and rs138183879 in *IKBKB*, through Sanger sequencing in 10 family members (A–J in Figure 1; Figure 4a). The rs138183879 SNP was not found in individual J, that is, it was not segregated with the disease in this family. In contrast, the novel mutation c.90263G>T in *TTN* was detected in all patients ($n=5$) and not detected in any of the unaffected family members ($n=5$) or 191 ethnically matched control subjects (382 chromosomes). These results suggested that this rare mutation in *TTN* segregated with the disease in this family.

DISCUSSION

In this study, we found that a novel missense mutation in *TTN* segregated with MFM in a large Japanese family. The identified c.90263G>T mutation in *TTN* (NM_001256850) was considered to be the genetic cause of MFM in our family, because (1) exome sequencing revealed that this was the best candidate mutation after filtering SNPs and indels, (2) this mutation is located in a region on chromosome 2 shared by affected family members, (3) the segregation with MFM was confirmed by Sanger sequencing, (4) this mutation was not detected in 191 control individuals, (5) this mutation was predicted to alter highly conserved amino acids (Figure 4b) and (6) *TTN* encodes a Z-disc-binding molecule called titin, which is similar to all of the previously identified causative genes for MFMs, which also encode Z-disc-associated molecules.

Recently, three mutations in *TTN* have been reported as the causes of hereditary myopathy with early respiratory failure (HMERF, MIM #603689),[11–16] which has similar muscle pathology to MFMs. The identified novel missense mutation c.90263G>T in our study was located on the same exon as recently reported HMERF mutations: c.90272C>T in a Portuguese family[16] and c.90315T>C in Swedish and English families[14,15] (Table 2). This finding suggests the possibility that our family can be recognized as having HMERF from a clinical aspect.

Compared with symptoms described in the past three reports on HMERF (also see Table 2), our patients have common features, such as autosomal dominant inheritance, early respiratory failure, the absence of clinically apparent cardiomyopathy, normal to mild elevation of serum CK and histological findings compatible with MFM. Early involvement of the tibialis anterior is also common, except for the Portuguese family, who reported isolated respiratory insufficiency and a milder presentation of HMERF. Thus, our family shares major clinical manifestations with patients with HMERF, suggesting that the identified mutation is novel for MFM and HMERF.

To date, mutations in *TTN* have been identified in skeletal myopathy and cardiomyopathy.[17,18] The relationship between the variant positions on *TTN* and phenotypes accompanied by skeletal or respiratory muscle involvement is summarized in Table 2. Titin is a large protein (4.20 MDa) that extends from the Z-disk to the M-line within the sarcomere, and it is composed of four major domains: Z-disc, I-band, A-band and M-line (Figure 5). All four HMERF mutations detected by other groups and our study were consistently located in the A-band domain, while mutations in tibial muscular dystrophy (TMD) (MIM #600334),[19–24] limb-girdle muscular dystrophy type 2J (LGMD2J) (#608807)[19,25] and early-onset myopathy with fatal cardiomyopathy (#611705)[26] were located in the M-line domain. HMERF and TMD have some common clinical characteristics, such as autosomal dominant inheritance with onset in adulthood and strong involvement of the tibialis anterior muscle.

Table 2 Previously reported TTN mutations with skeletal and/or respiratory muscle involvement

Phenotype	*LGMD*	*HMERF*	*Our family*	*HMERF*	*HMERF*	*TMD*	*TMD*	*LGMD2J*	*TMD*	*TMD*	*TMD*	*TMD*	*TMD*	*Early-onset myopathy with fatal cardiomyopathy*	*Early-onset myopathy with fatal cardiomyopathy*
Reported by	Vasli *et al.*[16]	Ohlsson *et al.*,[14] Pfeffer *et al.*[15]	Abe *et al.*[5]	Vasli *et al.*[16]	Edstrom *et al.*,[12] Nicolao, *et al.*[11] Lang e *et al.*[13]	Hackman *et al.*[23]	Udd *et al.*,[20] Hackman *et al.*[19]	Udd *et al.*,[25] Hackman *et al.*[19]	Pollazzon *et al.*[24]	Van den Bergh *et al.*[22]	Seze *et al.*,[21] Hackman *et al.*[19]	Hackman *et al.*[23]	Hackman *et al.*[23]	Carmignac *et al.*[26]	Carmignac *et al.*[26]
Mutation identified in Nucleotide (NM_001256850.1)	2012 c.3100G>A, c.52024G>A	2012 c.90315T>C	2012 c.90263G>T	2012 c.90272C>T	2005 c.97348C>T	2008 c.102724delT	2002 102857_ 102867 del11ins11	2002 102857_ 102867 del11ins11	2010 c.102914A>C	2003 c.102917T>A	2002 c.102944T>C	2008 c.102966delA	2008 c.102967C>T	2007 g.289385del ACCAAGTG	2007 g.291297delA
Protein (NP_001243779.1)	p.V1034M, p.A17342T	p.C30071R	p.W30088L	p.P30091L	p.R32450W				p.H34305P	p.I34306N	p.L34315P		p.Q34323X		
Domain	I-band, A-band	A-band (Fn3)	A-band (Fn3)	A-band (Fn3)	A-band (kinase)	M-line	M-line	M-line	M-line	M-line	M-line	M-line	M-line	M-line	M-line
Population	French	Swedish English	Japanese	Portuguese	Swedish	French	Finnish	Finnish	Italian	Belgian	French	Spanish	French	Sudanese	Moroccan
Inheritance	AR	AD	AD	AD	AD	AD	AD	AR	AD	AD	AD	AD	AD	Consanguineous siblings	Consanguineous siblings
Onset	35	33–71	27–45	46	20–50s	20–30s	35–55	20–30s	50–60s	47	45	40–50s	30s	Neonatal	Infant-early childhood
Skeletal muscles															
Major	Proximal UL and LL	TA, PL, EDL, ST	TA, ST	No	TA, neck flexor, proximals	TA, GA,HAM, pelvic	TA	All proximals	TA	TA	TA	TA	TA, HAM, pelvic	General muscle weakness and hypotonia	Psoas, TA, GA, peroneus
Minor		Neck flexor	Cervical, shoulder girdles, intercostals, proximal limb			QF				EDL, peroneal, TP	GA, femoral, scapular	HAM, GA	GA, distal UL		QF, proximal UL, neck, facial, trunk flexor
Spared			Facial			Proximal UL	Facial, UL, proximals	Facial		UL, proximal LL	Facial	UL	Proximal UL, QF		
Cardiac muscles	ND	No	No	ND	ND	ND	No	No	ND	ND	ND	ND	ND	DCM, onset; in the first decade	DCM, onset; 5–12 years old
Respiratory failure	ND	Yes, within 5–8 years	Yes, within 7 years	Isolated respiratory failure	Yes, as first presentation	ND	ND	ND	ND	ND	ND	ND	ND	ND	ND
Muscle pathologic features	ND	Inclusion bodies (major) and RVs (minor)	Cytoplasmic bodies (major) and RVs (minor)	Cytoplasmic bodies	Cytoplasmic bodies, positive for rhodamine-conjugated phalloidin	Dystrophic pattern without vacuoles	Nonspecific dystrophic change	Nonspecific dystrophic change, loss of calpain-3	Dystrophic pattern with RVs	Nonspecific, RV	Nonspecific	Dystrophic pattern with RVs	Nonspecific	Minicore-like lesions and abundant central nuclei	Minicore-like lesions and abundant central nuclei

Abbreviations: AD, autosomal dominant; AR, autosomal recessive; DCM, dilated cardiomyopathy; EDL, extensor digitorum longus; GA, gastrocnemius; HAM, hamstrings; LL, lower limb; ND, not described; no, no involvement; PL, peroneus longus; QF, quadriceps femoris; RV, rimmed vacuole;
ST, semitendinosus; TA, tibialis anterior; TMD, tibial muscular dystrophy; TP, tibialis posterior; UL, upper limb.

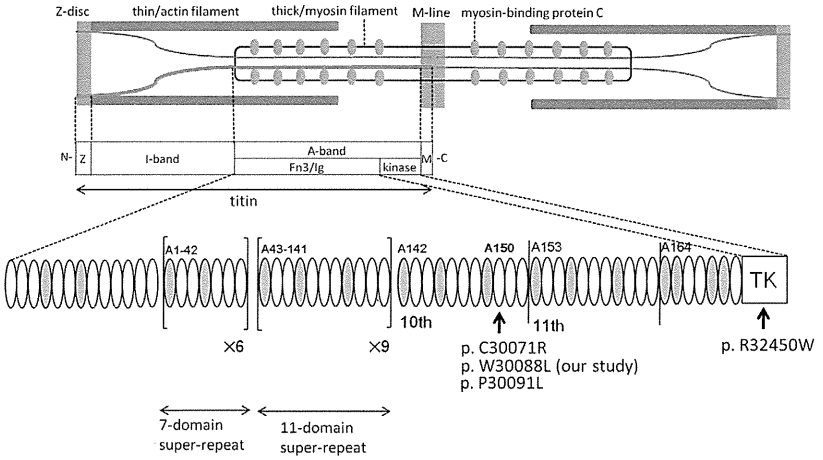

Figure 5 Structure of titin and mutation distribution in the A-band domain. Human *TTN* was mapped to 2q31.2. *TTN* is 294 kb and is composed of 363 exons that code for a maximum of 38 138 amino-acid residues and a 4.20-MDa protein[32] called titin. Titin is expressed in the cardiac and skeletal muscles and spans half the sarcomere, with its N-terminal at the Z-disc and the C-terminal at the M-line.[33] Titin is composed of four major domains: Z-disc, I-band, A-band and M-line. I-band regions of titin are thought to make elastic connections between the thick filament (that is, myosin filament) and the Z-disc within the sarcomere, whereas the A-band domain of titin seems to be bound to the thick filament, where it may regulate filament length and assembly.[34] The gray and white ellipses indicate an Ig-like domain and fibronectin type 3 domain, respectively. Our mutation (p.W30088L) and the neighboring two mutations (that is, p.C30071R and p.P30091L) were all located in the 6th Fn3 domain in the 10th domain of large super-repeats. A full color version of this figure is available at the *Journal of Human Genetics* journal online.

In contrast, one of the distinctive features of TMD is that early respiratory failure has not been observed in patients with TMD. Histological findings of TMD usually do not include CBs but show nonspecific dystrophic change. The underlying pathogenic processes explaining why mutations on these neighboring domains share some similarities but also some differences are unknown.

Three of four HMERF mutations in the A-band domain are located in the fibronectin type 3 and Ig-like (Fn3/Ig) domain, and one of four HMERF mutations is located in the kinase domain (Table 2, also see Figure 5). The missense mutation c.97348C>T in the kinase domain was the first reported HMERF mutation. It has been shown that the kinase domain has an important role in controlling muscle gene expression and protein turnover via the neighbor of BRCA1 gene-1-muscle-specific RING finger protein-serum response transcription factor pathway.[13] Moreover, the Fn3/Ig domain is composed of two types of super-repeats: six consecutive copies of 7-domain super-repeat at the N-terminus and 11 consecutive copies of 11-domain super-repeat at the C-terminus.[27–29] These super-repeats are highly conserved among species and muscles. Our identified mutation (c.90263G>T) and the neighboring two mutations (that is, c.90272C>T and c.90315T>C shown in Table 2) were all located on the 6th Fn3 domain in the 10th copy of 11-domain super-repeat (that is, A150 domain[30]) (Figure 5). Although some Fn3 domains are proposed to be the putative binding site for myosin,[31] the role with the majority of Fn3 domains, how it supports the structure of each repeat architecture, and the identity of its binding partner have not been fully elucidated. Our findings suggested that the Fn3 domain, in which mutations clustered, has critical roles in the pathogenesis of HMERF, although detailed mechanisms of pathogenesis remain unknown.

In conclusion, we have identified a novel disease-causing mutation in *TTN* in a family with MFM that was clinically compatible with HMERF. Because of its large size, global mutation screening of *TTN* has been difficult. Mutations in *TTN* may be detected by massively parallel sequencing in more patients with MFMs, especially in patients with early respiratory failure. Further studies are needed to understand the genotype–phenotype correlations in patients with mutations in *TTN* and the molecular function of titin.

ACKNOWLEDGEMENTS

We thank the patients and their family. We are grateful to Yoko Tateda, Kumi Kato, Naoko Shimakura, Risa Ando, Riyo Takahashi, Miyuki Tsuda, Nozomi Koshita, Mami Kikuchi and Kiyotaka Kuroda for their technical assistance. We also acknowledge the support of the Biomedical Research Core of Tohoku University Graduate School of Medicine. This work was supported by a grant of Research on Applying Health Technology provided by the Ministry of Health, Labor and Welfare to YM, an Intramural Research Grant (23-5) for Neurological and Psychiatric Disorders of NCNP and JSPS KAKENHI Grant number 24659421.

1 Nakano, S., Engel, A. G., Waclawik, A. J., Emslie-Smith, A. M. & Busis, N. A. Myofibrillar myopathy with abnormal foci of desmin positivity. I. Light and electron microscopy analysis of 10 cases. *J. Neuropathol. Exp. Neurol.* **55,** 549–562 (1996).
2 Olive, M., Odgerel, Z., Martinez, A., Poza, J. J., Bragado, F. G., Zabalza, R. J. *et al.* Clinical and myopathological evaluation of early- and late-onset subtypes of myofibrillar myopathy. *Neuromuscul. Disord.* **21,** 533–542 (2011).
3 Olive, M., Goldfarb, L. G., Shatunov, A., Fischer, D. & Ferrer, I. Myotilinopathy: refining the clinical and myopathological phenotype. *Brain* **128,** 2315–2326 (2005).
4 Selcen, D. & Engel, A. G. Myofibrillar myopathy caused by novel dominant negative alpha B-crystallin mutations. *Ann. Neurol.* **54,** 804–810 (2003).
5 Abe, K., Kobayashi, K., Chida, K., Kimura, N. & Kogure, K. Dominantly inherited cytoplasmic body myopathy in a Japanese kindred. *Tohoku. J. Exp. Med.* **170,** 261–272 (1993).
6 Abecasis, G. R., Cherny, S. S., Cookson, W. O. & Cardon, L. R. Merlin–rapid analysis of dense genetic maps using sparse gene flow trees. *Nat. Genet.* **30,** 97–101 (2002).
7 Li, H. & Durbin, R. Fast and accurate short read alignment with Burrows-Wheeler transform. *Bioinformatics* **25,** 1754–1760 (2009).
8 McKenna, A., Hanna, M., Banks, E., Sivachenko, A., Cibulskis, K., Kernytsky, A. *et al.* The Genome Analysis Toolkit: a MapReduce framework for analyzing next-generation DNA sequencing data. *Genome. Res.* **20,** 1297–1303 (2010).
9 Wang, K., Li, M. & Hakonarson, H. ANNOVAR: functional annotation of genetic variants from high-throughput sequencing data.. *Nucleic Acids Res.* **38,** e164 (2010).
10 Adzhubei, I. A., Schmidt, S., Peshkin, L., Ramensky, V. E., Gerasimova, A., Bork, P. *et al.* A method and server for predicting damaging missense mutations. *Nat. Methods* **7,** 248–249 (2010).
11 Nicolao, P., Xiang, F., Gunnarsson, L. G., Giometto, B., Edstrom, L., Anvret, M. *et al.* Autosomal dominant myopathy with proximal weakness and early respiratory muscle involvement maps to chromosome 2q. *Am. J. Hum. Genet.* **64,** 788–792 (1999).

12 Edstrom, L., Thornell, L. E., Albo, J., Landin, S. & Samuelsson, M. Myopathy with respiratory failure and typical myofibrillar lesions. *J. Neurol. Sci.* **96,** 211–228 (1990).
13 Lange, S., Xiang, F., Yakovenko, A., Vihola, A., Hackman, P., Rostkova, E. *et al.* The kinase domain of titin controls muscle gene expression and protein turnover. *Science* **308,** 1599–1603 (2005).
14 Ohlsson, M., Hedberg, C., Bradvik, B., Lindberg, C., Tajsharghi, H., Danielsson, O. *et al.* Hereditary myopathy with early respiratory failure associated with a mutation in A-band titin. *Brain* **135,** 1682–1694 (2012).
15 Pfeffer, G., Elliott, H. R., Griffin, H., Barresi, R., Miller, J., Marsh, J. *et al.* Titin mutation segregates with hereditary myopathy with early respiratory failure. *Brain* **135,** 1695–1713 (2012).
16 Vasli, N., Bohm, J., Le Gras, S., Muller, J., Pizot, C., Jost, B. *et al.* Next generation sequencing for molecular diagnosis of neuromuscular diseases. *Acta. Neuropathol.* **124,** 273–283 (2012).
17 Kontrogianni-Konstantopoulos, A., Ackermann, M. A., Bowman, A. L., Yap, S. V. & Bloch, R. J. Muscle giants: molecular scaffolds in sarcomerogenesis. *Physiol. Rev.* **89,** 1217–1267 (2009).
18 Ottenheijm, C. A. & Granzier, H. Role of titin in skeletal muscle function and disease. *Adv. Exp. Med. Biol.* **682,** 105–122 (2010).
19 Hackman, P., Vihola, A., Haravuori, H., Marchand, S., Sarparanta, J., De Seze, J. *et al.* Tibial muscular dystrophy is a titinopathy caused by mutations in TTN, the gene encoding the giant skeletal-muscle protein titin. *Am. J. Hum. Genet.* **71,** 492–500 (2002).
20 Udd, B., Partanen, J., Halonen, P., Falck, B., Hakamies, L., Heikkila, H. *et al.* Tibial muscular dystrophy. Late adult-onset distal myopathy in 66 Finnish patients. *Arch. Neurol.* **50,** 604–608 (1993).
21 de Seze, J., Udd, B., Haravuori, H., Sablonniere, B., Maurage, C. A., Hurtevent, J. F. *et al.* The first European family with tibial muscular dystrophy outside the Finnish population. *Neurology* **51,** 1746–1748 (1998).
22 Van den Bergh, P. Y., Bouquiaux, O., Verellen, C., Marchand, S., Richard, I., Hackman, P. *et al.* Tibial muscular dystrophy in a Belgian family. *Ann. Neurol.* **54,** 248–251 (2003).
23 Hackman, P., Marchand, S., Sarparanta, J., Vihola, A., Penisson-Besnier, I., Eymard, B. *et al.* Truncating mutations in C-terminal titin may cause more severe tibial muscular dystrophy (TMD). *Neuromuscul. Disord.* **18,** 922–928 (2008).
24 Pollazzon, M., Suominen, T., Penttila, S., Malandrini, A., Carluccio, M. A., Mondelli, M. *et al.* The first Italian family with tibial muscular dystrophy caused by a novel titin mutation. *J. Neurol.* **257,** 575–579 (2010).
25 Udd, B., Rapola, J., Nokelainen, P., Arikawa, E. & Somer, H. Nonvacuolar myopathy in a large family with both late adult onset distal myopathy and severe proximal muscular dystrophy. *J. Neurol. Sci.* **113,** 214–221 (1992).
26 Carmignac, V., Salih, M. A., Quijano-Roy, S., Marchand, S., Al Rayess, M. M., Mukhtar, M. M. *et al.* C-terminal titin deletions cause a novel early-onset myopathy with fatal cardiomyopathy. *Ann. Neurol.* **61,** 340–351 (2007).
27 Labeit, S., Barlow, D. P., Gautel, M., Gibson, T., Holt, J., Hsieh, C. L. *et al.* A regular pattern of two types of 100-residue motif in the sequence of titin. *Nature* **345,** 273–276 (1990).
28 Labeit, S. & Kolmerer, B. Titins: giant proteins in charge of muscle ultrastructure and elasticity. *Science* **270,** 293–296 (1995).
29 Tskhovrebova, L., Walker, M. L., Grossmann, J. G., Khan, G. N., Baron, A. & Trinick, J. Shape and flexibility in the titin 11-domain super-repeat. *J. Mol. Biol.* **397,** 1092–1105 (2010).
30 Bucher, R. M., Svergun, D. I., Muhle-Goll, C. & Mayans, O. The structure of the FnIII Tandem A77-A78 points to a periodically conserved architecture in the myosin-binding region of titin. *J. Mol. Biol.* **401,** 843–853 (2010).
31 Muhle-Goll, C., Habeck, M., Cazorla, O., Nilges, M., Labeit, S. & Granzier, H. Structural and functional studies of titin's fn3 modules reveal conserved surface patterns and binding to myosin S1–a possible role in the Frank-Starling mechanism of the heart. *J. Mol. Biol.* **313,** 431–447 (2001).
32 Bang, M. L., Centner, T., Fornoff, F., Geach, A. J., Gotthardt, M., McNabb, M. *et al.* The complete gene sequence of titin, expression of an unusual approximately 700-kDa titin isoform, and its interaction with obscurin identify a novel Z-line to I-band linking system. *Circ. Res.* **89,** 1065–1072 (2001).
33 Maruyama, K., Yoshioka, T., Higuchi, H., Ohashi, K., Kimura, S. & Natori, R. Connectin filaments link thick filaments and Z lines in frog skeletal muscle as revealed by immunoelectron microscopy. *J. Cell. Biol.* **101,** 2167–2172 (1985).
34 Guo, W., Bharmal, S. J., Esbona, K. & Greaser, M. L. Titin diversity–alternative splicing gone wild. *J. Biomed. Biotechnol.* **2010,** 753675 (2010).

Supplementary Information accompanies the paper on Journal of Human Genetics website (http://www.nature.com/jhg)